Modeling of Spur Gear Meshing Characteristics under Various Crack Size

By

Sofuan Najen Bin Othman

Dissertation submitted in partial of the requirement for the

Mechanical Engineering (Hons)

(Mechanical Engineering Department)

MAY 2012

Universiti Teknologi PETRONAS
Bandar Seri Iskandar
31750 Tronoh
Perak Darul Ridzuan.

CERTIFICATION OF APPROVAL

Modeling of Spur Gear Meshing Characteristics under Various Crack Size

By

Sofuan Najen B. Othman

A project dissertation submitted to the
Mechanical Engineering Programme
Universiti Teknologi PETRONAS
in partial fulfillment of the requirement for the
BACHELOR OF ENGINEERING (Hons)
(MECHANICAL ENGINEERING)

Approved by,

_____

(Ir. Idris bin Ibrahim)

UNIVERSITI TEKNOLOGI PETRONAS
TRONOH, PERAK
May 2012

CERTIFICATION OF ORIGINALITY

This is to certify that I am responsible for the work submitted in this project, that the original work is my own except as specified in the references and acknowledgements, and that the original work contained herein have not been undertaken or done by unspecified sources or persons.

_____

SOFUAN NAJEN BIN OTHMAN

ABSTRACT

This report focused on the study of gear defect based on the gear meshing stiffness variation. The main objective of this study is to investigate the gear defect by modeling the gear based on the gear material and gear parameter. The main failure that occurs to gear is crack defect due to concentration of stress at the root of gear tooth. The crack cannot be detected because gear located at the middle of the system and the size of crack is too small to be seen with naked eyes. The crack also will affect the total gear meshing stiffness, which causes it to reduce drastically. The work focused on modeling the gear using different type of materials, which are mild steel and Aluminum S6061 to study the different characteristic of gear meshing stiffness. It also includes the modeling of the gear with various crack size to compare thetrend of the gear meshing stiffness.

The research methodology adopted involves modeling the healthy gear which is gear without defect for baseline data. The total meshing stiffness is the summation of the Hertzian contact, shear, bending and axial contact stiffnesses. The meshing period is calculated to differentiate between single and double meshing tooth. All the calculation is done using MATLAB software which is very handy in solving complex equations. The method adopted in this project was originally developed by Tian and it is also known as the Tian's method. The vibration characteristic for the healthy gear resulted from the simulation is validated with the experimental data afterwhich the work proceeded to modeling the gear with various crack size ranging from 0.0014mm to 0.005mm. The gear with broken tooth is also modeled to review the characteristic of missing tooth gear stiffness.

It can be concluded that the crack would cause the reduction of gear meshing stiffness. The initiation of crack propagation will cause the changes in shear and bending stiffness thus changes the overall total gear meshing stiffness. Materials such as steel and Aluminum has different value of Young Modulus and it causes the different of total gear meshing stiffness. The size of crack also affects the meshing stiffness. If the crack size is bigger, the total gear meshing stiffness will be smaller.

ACKNOWLEDGEMENT

First of all, I would like to express my gratitude to my beloved creator, Allah S.W.T for guiding me throughout my entire study and giving me strength in completing my Final Year Project.

I also would like to thank Ir. Idris B. Ibrahim for his support and idea for the whole two semesters in order to ensure the success of the project.

On top of that, I am also appreciating Mr. TamiruAlemu for teaching and guiding me on how to write Mathlab codes correctly.

To Mr. Rizal Lias, I would like to thank for sharing his knowledge on ANSYS software, teaching of dynamic of gear behavior and sharing some data related to gear design.

Finally, I would like to express my gratitude and expression to all my friends for supporting me since the start of this project. It is pleasure to get working with all of them for project completion.

TABLE OF CONTENT

LIST OF FIGURES

LIST OF FIGURES

LIST OF TABLES

LIST OF SYMBOLS

Symbol	Description
F	Elastic contact force
d	Distance between contact point and tooth root
x	Distance from tooth root
h	Distance between contact point and tooth's central line
α_1	Angle between line O_1C and tooth central line
α_2	$\alpha_2 = \frac{\pi}{2N} + \tan\alpha_0 - \alpha_0$
M	Bending effect
N_1	Pinion teeth
N_2	Gear teeth
I_x	Area moment of inertia
U_s	Potential energy stored during shearing
α_0	Pressure angle
k_t	Total stiffness
k_h	Hertzian contact stiffness
k_s	Shear stiffness
k_a	Axial compressive stiffness
E	Young's modulus
L	Tooth width
ν	Poisson's ratio
G	Shear modulus
A_x	Area of the section
U_a	Potential energy stored during axial compressive

CHAPTER 1

INTRODUCTION

1.1 Background of Study

Nowadays, gear can be considered as the most important part in machinery world. There are various types of gears that have been used in all machines such as external and internal gear, spur gear, helical gear, skew gear and crown gear. The functions of gear are to reduce rotational speed, increasing available torque and changing the direction of power transmission. Despite of many functions, there is one major problem that can cause huge lost in industrial field which is the failure of gear. Sudden failure of the gear may not just cause the decreasing of the efficiency but also can cause the stoppage of the machine. This effect also can cause fatality. For example, if a person is driving a car at high speed and suddenly the gearbox fail. He/she might lose control of his/her vehicle and it will lead to accident. In the nutshell, the analysis of gear defect is very important to detect the defect and also estimate the fatigue life of the gear. There are several modes of defects such as scoring, wear, pitting and crack. In this project analysis, crack defects will be considered in order to model the gear meshing characteristic that caused by the defects of the gear. Meanwhile, crack initiate at the weakest point of the teeth usually happen at the root of tooth because of high stress concentration. The crack will propagate fast and will result tooth fracture. This will cause the decreasing efficiency of the system.

1.2 Problem Statement

The main concern is the sudden failure of the gear due to common defect such as pitting, crack propagation and wear. The broken gear teeth are due to fast crack propagation. When the initial crack and pitting occur at the gear teeth, the meshing stiffness will decrease and the bending deflection will increase. So, analysis of the defect was done in order to determine the meshing characteristics at the gear teeth. Many studies have been

done mostly by using Finite Element Analysis. Since the method was quite expensive and very difficult to model, the other alternative was by using analytical model which can analyze the meshing stiffness characteristic of the gear. Base equation was developed in order to differentiate between the meshing characteristics of normal spur gear and defect spur gear.

1.3 Objective

The main objective of this project is to investigate the defect that occurs at gear especially at the teeth of the gear by analyzing the gear meshing characteristic under various sizes of crack. To analyze the difference between of all the data that was calculated, the baseline data would be modeled by developing equation of total meshing gear stiffness for spur gear (without defect). Analysis and equations that would be developed for the mathematical modeling include:

1. Developed the mathematical model of gear by using mesh stiffness method for normal gear.
2. The normal gear model would be compared to defect gear by comparing the trend of total gear meshing stiffness.

1.4 Scope of Study

This project covered mostly on the kinematic of gear, meshing stiffness and cracking analysis. At the end of this project, the result would be presented by simulation of data in mathematical model equation. All the data were compared with experimental value to see the accuracy of the gear modeling. For this project, the mathematical model was not analyzing the external effect such as viscous damping that provide by lubricant, wear of tooth gear and surface friction of the tooth. And the data were changed based on type of material and gear to calculate for the different number of tooth. Type of the material also will be considered to relate with the rate of crack propagation.

CHAPTER 2

LITERATURE REVIEW

Many studies have been carried out in order to investigate the fatigue life of spur gear. Most of the studies are focus on the vibration of the gear, the reduction of the gear meshing stiffness and dynamic of the gear. For this project, it will mainly cover on the reduction of the meshing stiffness due to crack propagation (Figure 2.1) and pitting (Figure 2.2) and also the vibration characteristics of the spur gear. All of this study will be presented by mathematical model. Ozguven et al. [1] had reviewed the mathematical models in gear dynamics which present the behavior of the gear dynamics without defects. On the other hand, Pareyet.al [2] suggests that accuracy of data on the gear vibration with defect can be obtained by following analytical procedure of gear dynamic model. There are several studies that had been done in order to calculate the mesh stiffness. The analytical method is very useful. It shows good result and strong agreement compared to FEM analysis [3].

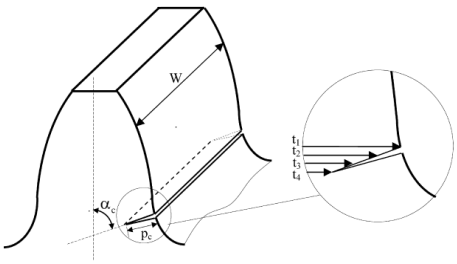

Figure 2.1: Crack defect [8]

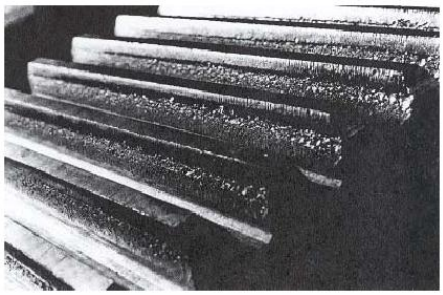

Figure 2.2: Pitting defect [8]

Pareyet. al [4] has built six-degree of freedom nonlinear model of gearbox which as in Figure 2.3. The model consists of two gears on the two shafts that are connected to a load and a prime mover. The model also consist of four inertias, namely load, prime mover, pinion and gear. Both bearing and shaft damping are considered in this model. The transverse vibrations of the gear are considered along the line of action. This model is very useful to get the response, including modulations due to transverse and torsional vibration stemming from bearing and shaft compliances that can be calculated

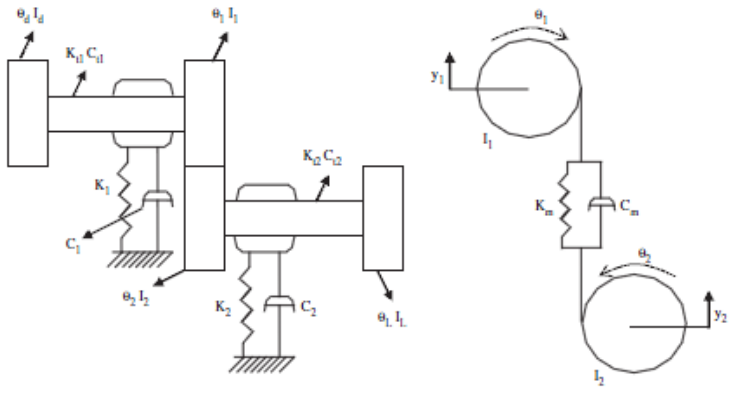

Figure 2.3: Six degree of freedom nonlinear model [4]

From the model, the governing equations of motion for six degree of freedom nonlinear model can be written as below [4]:

$$I_D\theta_D'' + c_{t1}(\theta_D' - \theta_1') + k_{t1}(\theta_D - \theta_1) = T_D \quad (1)$$

$$I_1\theta_1'' + c_{t1}(\theta_1' - \theta_D') + k_{t1}(\theta_1 - \theta_D) = -W_0R_1 \quad (2)$$

$$I_2\theta_2'' + c_{t2}(\theta_2' - \theta_L') + k_{t2}(\theta_2 - \theta_L) = W_0R_2 \quad (3)$$

$$I_L\theta_L'' + c_{t2}(\theta_L' - \theta_2') + k_{t2}(\theta_L - \theta_2) = -T_L \quad (4)$$

$$m_1y_1'' + c_1y_1' + k_1y_1 = W_0 \quad (5)$$

$$m_2y_2'' + c_2y_2' + k_2y_2 = -W_0 \quad (6)$$

$W_0$is the dynamic mesh force:

$$W_0 = k_m(\theta_1R_1 - \theta_2R_2 + y_2 - y_1) + c_m(\theta_1'R_1 - \theta_2'R_2 + y_2' - y_1') \quad (7)$$

Every pair of gear system will have rectangular pulse s due to deformation and elasticity of the contacting components. To model the signal, half-sine pulses are considered. The response of the system can be represented by decaying sinusoid as shown in Figure 2.4.

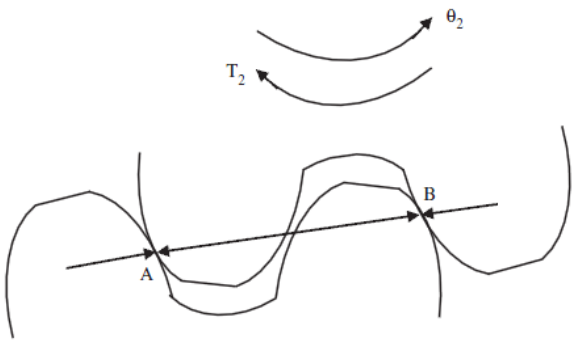

Figure 2.4: Response of a decaying half-sine pulse train [4]

In Figure 2.4, the double pair of tooth meshing. Single and double pair of tooth meshing occurs alternately. Point A and B are the contact point between teeth. The response of the decaying half-sine pulse train:

$$x(t) = (K/\sqrt{1-\zeta^2})e^{-\zeta\omega_0 t}sin\left\{\sqrt{1-\zeta^2}\omega_0 t + sin^{-1}(2\zeta\sqrt{1-\zeta^2})\right\} \qquad (8)$$

$K = k/\sqrt{1-\zeta^2}$where$k$ is the height of the pulse, ζ is damping ratio; frequency that generated pulse, $\omega_0 = \Pi/\Delta t$; pulse width $\Delta t = b/v_a$; b is the defect width in profile direction and v_a is the velocity at defect point. The differential equation (1)-(6) can be solved by using MATLAB and the result of the response is obtained as in Figure 2.5.

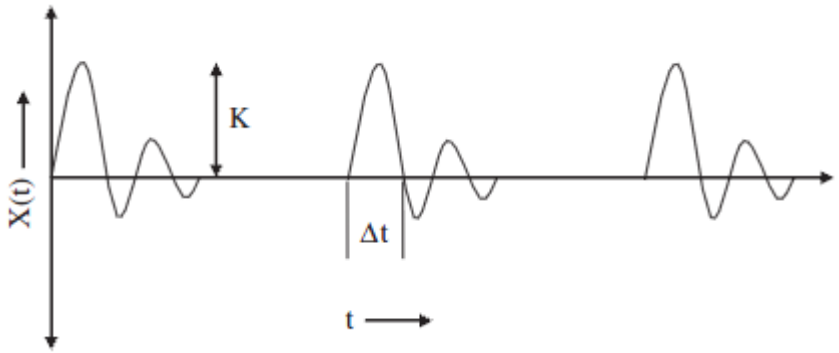

Figure 2.5: Two teeth pairs of spur gear in contact. [4]

Embedded model also can be useful to identify gear meshing stiffness. Lee et al. [5] has developed an embedded modeling of gear to identify the gear meshing stiffness from measuring gear angular displacement and proceed with embedded-dynamic-fracture model to predict gear fatigue crack propagation [6].The study of defect by determining the mesh stiffness also has been done by Chen [7] which develop an analytical model of mesh stiffness for spur gear pair to predict the tooth crack which propagates along both tooth width and crack depth. This model also can be used to assess the impact of gear tooth crack with different sizes on the gear mesh stiffness and the corresponding dynamic responses, which is useful

There is study to compare between the analytical data with FEA. Fakher [8] has done the comparison between the analytical modeling of crack propagation with the finite element analysis in term of time varying gear mesh stiffness. In this journal, the method that had been used is gear mesh stiffness analytical formulation, analytical modeling of tooth crack, finite element modeling, time varying gear stiffness and numerical simulation. Based on the result, the different between analytical model and FEA is not too obvious.

In this article, the authors state that gear mesh stiffness is a time varying parameter that reflects gear mesh conditions as the number of teeth contact varies and the line of contact of the engaged gear teeth also varies. The stiffness of one tooth can by considering by three factors which are bending deflectionδ_b, fillet foundation deflections δ_f and contact deflectionδ_h. For the study, the authors neglect the torsional mesh stiffness.

In Figure 2.6 modeled by Fakher [8] shows the location base of circle, dedendum and addendum. The height of tooth represented by L_c. F is the force that provided by motor. This value can be varies base on the speed of the motor. α_m is the pressure angle. Most of the gear that is fabricated has the value of 20^o.

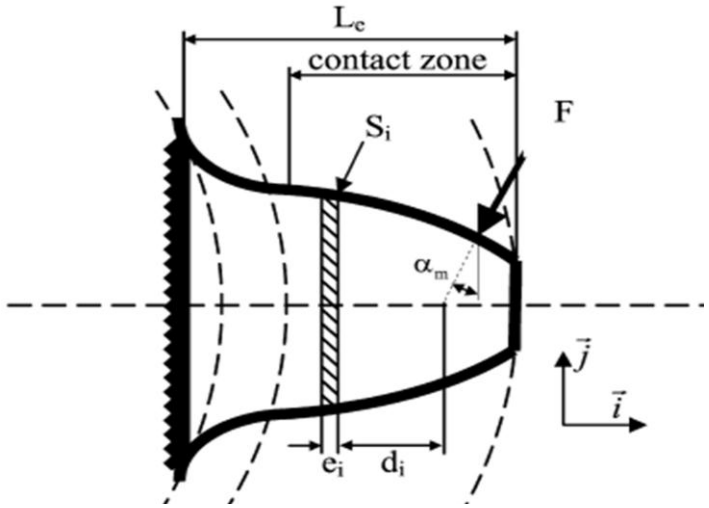

Figure 2.6: Modeling of spur gear tooth as a non-uniform cantilever beam [8]

For the bending deflection, the formula is:

$$\delta_b = F\cos^2\alpha_m \sum_{i=1}^{n} e_i \left\{ \frac{d_i - e_i d_i + \frac{1}{3}e_i^2}{E'\bar{I}_i} + \frac{1}{s_h G \bar{A}_i} + \frac{tan^2\alpha_m}{\bar{A}_i E'} \right\} \quad (2.1)$$

For the fillet foundation deflection, the formula is:

$$\delta_f = \frac{F\cos^2\alpha_m}{WE} \left\{ L^* \left(\frac{u_f}{S_f}\right)^2 + M^* \left(\frac{u_f}{S_f}\right) + P^*(1 + Q^* tg^2\alpha_m) \right\} \quad (2.2)$$

To solve this equation, the value of L, M, P and Q are needed as in the Table 2.1.

Table 2.1: Values of coefficients [4]

	A_i	B_i	C_i	D_i	E_i	F_i
$L^*(h_{fi}, \theta_f)$	-5.574×10^{-5}	-1.9986×10^{-3}	-2.301×10^{-4}	4.7702×10^{-3}	0.0271	6.8045
$M^*(h_{fi}, \theta_f)$	60.111×10^{-5}	28.1×10^{-3}	-84.431×10^{-4}	-9.926×10^{-3}	0.1624	0.9086
$P^*(h_{fi}, \theta_f)$	-50.95×10^{-5}	185.5×10^{-3}	0.0054×10^{-4}	53.3×10^{-3}	0.2895	0.9236
$Q^*(h_{fi}, \theta_f)$	-6.204×10^{-5}	9.0889×10^{-3}	-4.0964×10^{-4}	7.8297×10^{-3}	-0.147	0.6904

For the contact deflection, the formula is:

$$k_h = \frac{\pi EW}{4(1-\nu^2)} \tag{2.3}$$

From the three deflections, the stiffness of each deflection can be calculated as:

$$Bendingstiffness, K_b = 1/\delta_b \tag{2.4}$$

$$Filletfoundationstiffness, K_f = 1/\delta_f \tag{2.5}$$

$$Contactstiffness, K_f = 1/\delta_h \tag{2.6}$$

The tooth pair gear mesh stiffness can be obtained by solving the summation of the equation:

$$K_{12} = \frac{1}{K_{b1}} + \frac{1}{K_{f1}} + \frac{1}{K_{b1}} + \frac{1}{K_{b2}} + \frac{1}{K_{f2}} + \frac{1}{K_h} \tag{2.7}$$

Numerical simulation has been done by authors to compare the result between Finite Element Analysis and analytical model. Two examples of crack propagation have been taken with different crack angle as shown in Figure 2.7.

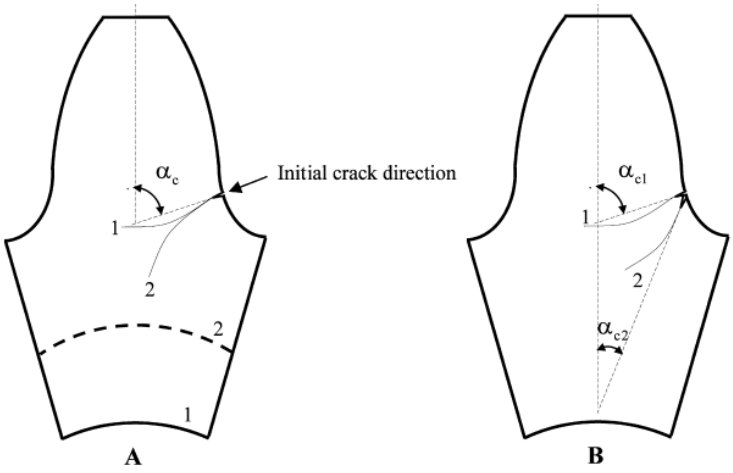

Figure 2.7: Influence of backup ratio (A) and initial crack angle (B) on crack propagation directions [8]

In early discussion, authors have stated that the Finite element analysis method can be replaced by analytical method in order to get the same result but easier method. The difference between analytical method and finite element analysis method can be as in Figure 2.8 where the difference between FEM and analytical model is too small. On top of that, the strong agreement between FEA and analytical method can be seen in Figure 2.9 where the graphs show the difference between the meshing stiffness of healthy gear and defect gear.

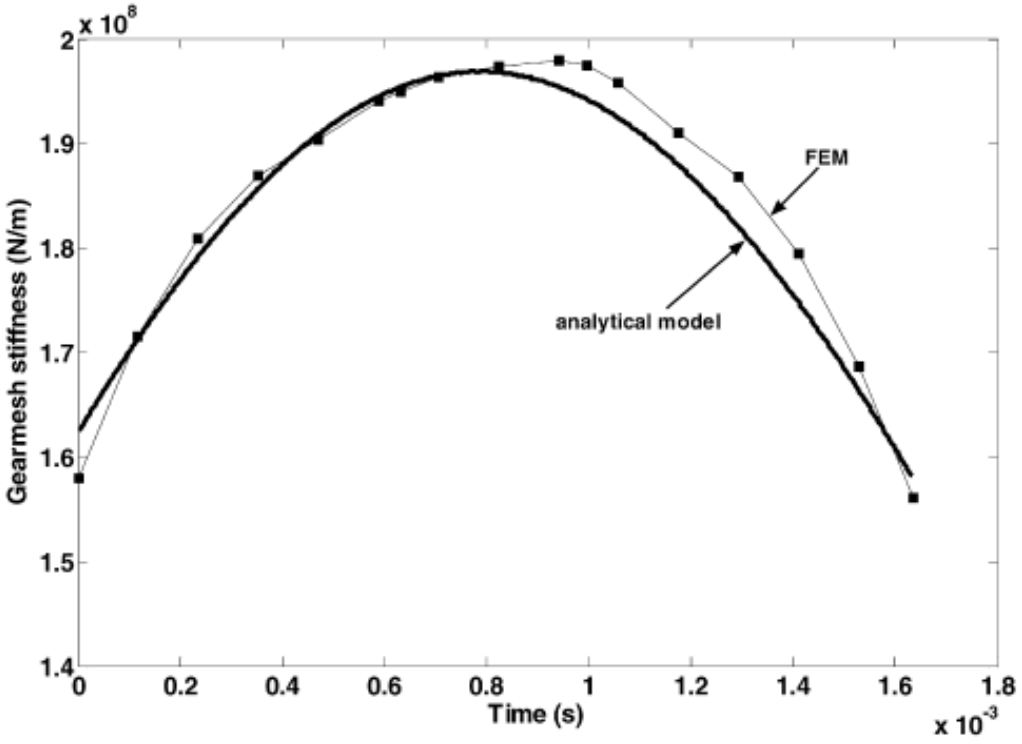

Figure 2.8: Evolution of K_{12} for healthy case. [8]

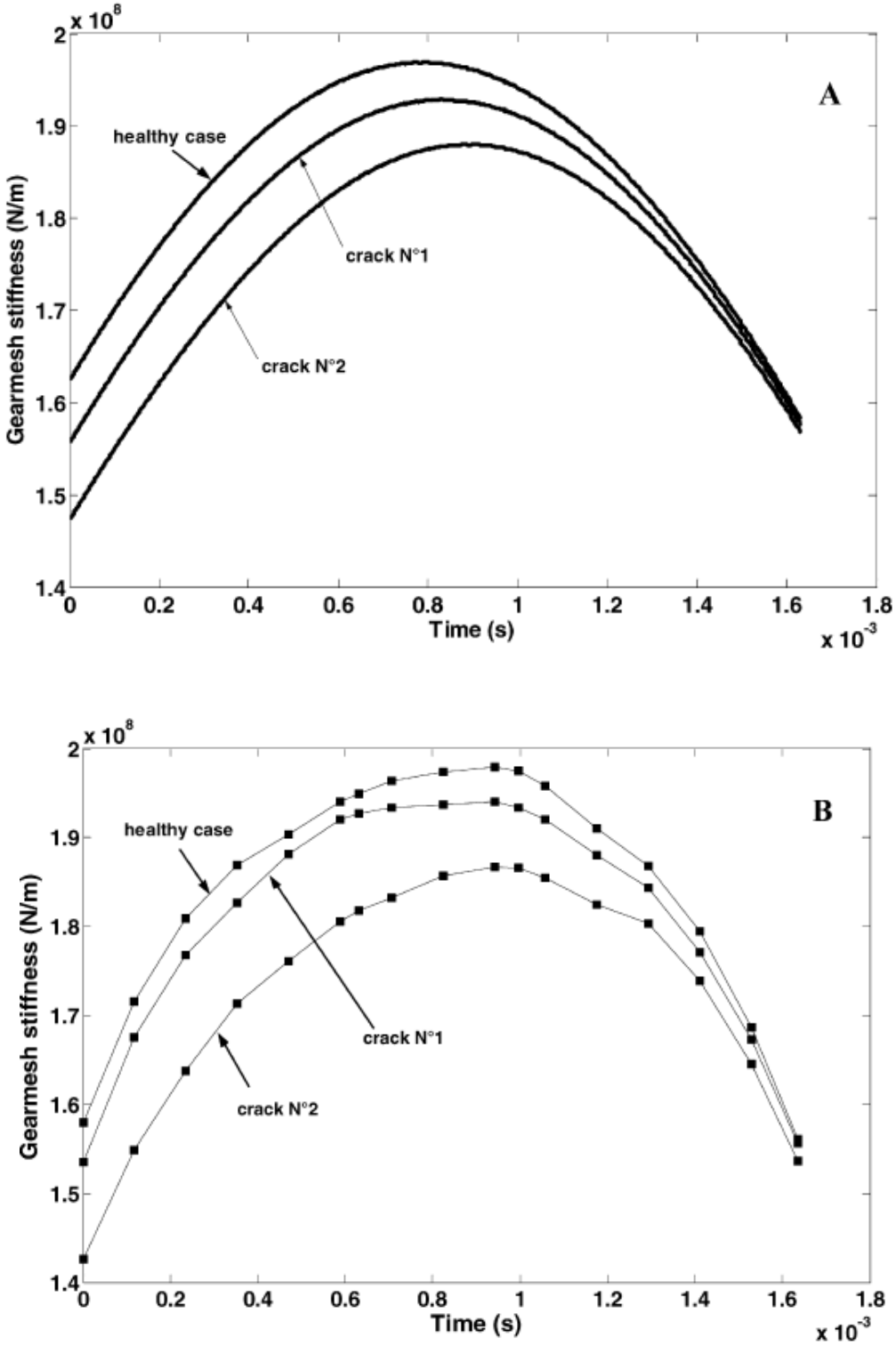

Figure 2.9: Evolution of K_{12} for the crack cases (A) Analytical model. (B) FEM [8

CHAPTER 3

METHODOLOGY

3.1 Flowchart of the analytical study on modeling spur gear meshing characteristics.

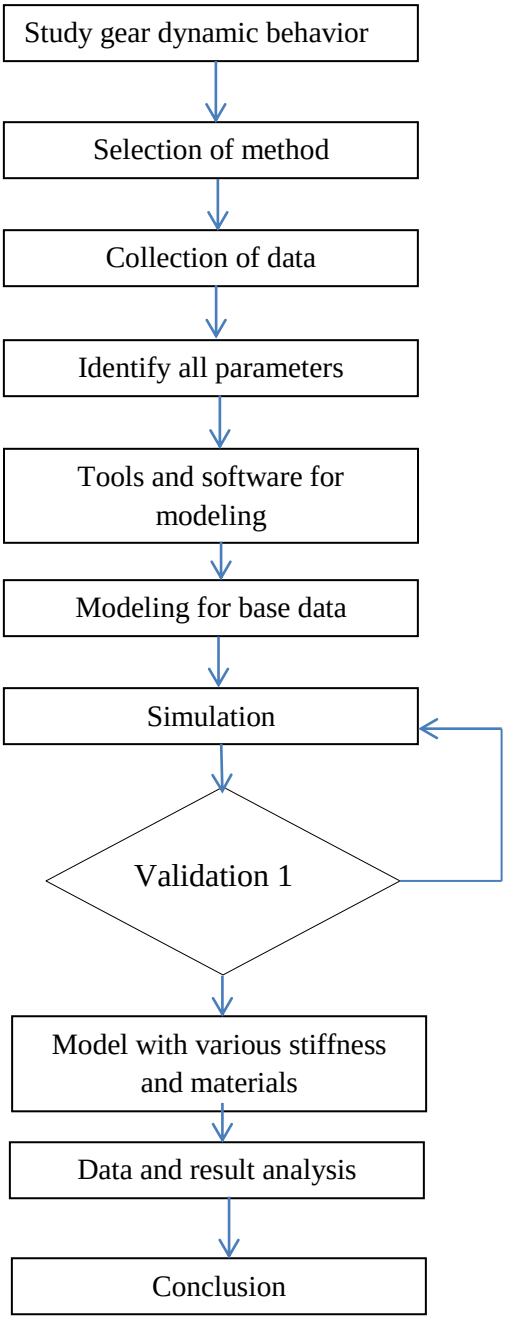

Figure 3.1: Flow chart of the project

3.2 Research Methodology

The Figure 3.1 is the flow chart for overall project flow. The main purpose of this project is to develop a mathematical equation for spur gear to detect any defect that occurs at the tooth of gear. For the first part of the project, the detail of gear dynamic behavior from mechanic of machine subject and also vibration characteristic that have been taught in vibration subject were studied. The next stage was finding the article that can be related to the gear defect and how to detect the defect at gear tooth. Many experiments related to spur gear defect analysis can be the foundation of this project. The best method need to be selected to ensure that the outcome result will be relevant. The method that has been selected is Tian's method which discusses in detail how to model the gear with crack defect. All the parameters that involve in spur gear equation needed to be identified in order to develop mathematical force function. This data collection took about 3 and half week.

The second stage of this project was to solve the mathematical equation that involve in the gear model. The equations were solved by using MATLAB software. For the first model, the parameter that provided in Tian's article was used. This was to see the result that Tian's obtained from his model. The model was simulated and the result was analyzed. Then, the parameter was changed by using parameter of UTP gear. Then, the model was simulated. Both of the results were compared to see the different. Base on the result that obtained from these models in chapter 4, the result was valid because the value by using UTP gear parameter and Tian's parameter was not too different. So, the method was preceded with crack defect model.

The third stage of the project was modeling the gear with crack propagation. The Tian's method was used in order to calculate the total gear meshing stiffness. The crack would cause the reduction to the total gear meshing stiffness. At this stage, four sizes of crack had been modeled which are crack with size 0.0014m, 0.003m, 0.005m and broken tooth. The results were compared to see the trend of gear meshing characteristic for each crack size. After obtaining and analyzing all the data, it can be concluded that the project meet the objectives.

Table 3.1: Tian's gear parameter

	Pinion	Gear
Teeth	Z_1=19	Z_2=48
Module (mm)	1	1
Teeth thickness (mm)	W=16	W=16
Rotational speed (rpm)	N_1=1000	N_2=570
Pressure angle	20^o	20^o
Young modulus E (N/mm^2)	2.068×10^{11}	2.068×10^{11}
Poisson's ration	0.3	0.3

Table 3.2: UTP gear parameter

	Pinion	Gear
Teeth	Z_1=100	Z_2=174
Module (mm)	1	1
Teeth thickness (mm)	W=10	W=10
Rotational speed (rpm)	N_1=1000	N_2=570
Pressure angle	20^o	20^o
Young modulus E (N/mm^2)	6.9×10^{10}	6.9×10^{10}
Poisson's ration	0.33	0.33

Table 3.1 is the parameter that was used in Tian's study. The total teeth for the pinion are 19 and the total teeth for gear are 48. Compared to UTP gear model in Table 3.2, the total teeth for pinion are 100 and total teeth and the total teeth for gear were 174. Both model used the same module which is 1 mm. the other different between these two models was the teeth thickness. The teeth thickness for Tian's model was 16mm meanwhile the UTP gear model was 10mm. The thickness of the teeth also would play a vital role to estimate the crack propagation. Tian's used mild steel to model the gear. The value of young modulus for mild steel is 2.068×10^{11}. UTP gear used Aluminum S6061 and the value for Young Modulus for Aluminum is 6.9×10^{10}. The value of Poisson's ratio for both model were different. For Tian's model, the Poisson ratio was 0.3 and the Poisson ratio for UTP gear model was 0.33. All the values in the tables would play the vital role in order to calculate the total meshing gear.

3.3 Project activities

In this section will be discussing the detail of methodology. The first activity was to model the base data for healthy gear. The first step in modeling was by calculating the gear mesh stiffness. As being discussed in literature review section and study the past research, gear mesh stiffness is very important in order to observe the vibration characteristics of meshing gear. The crack propagation can reduce the meshing stiffness. So, there are 3 types of deflection that will be considered to calculate the gear mesh stiffness. The detail of gear can be described as in Figure 3.2.

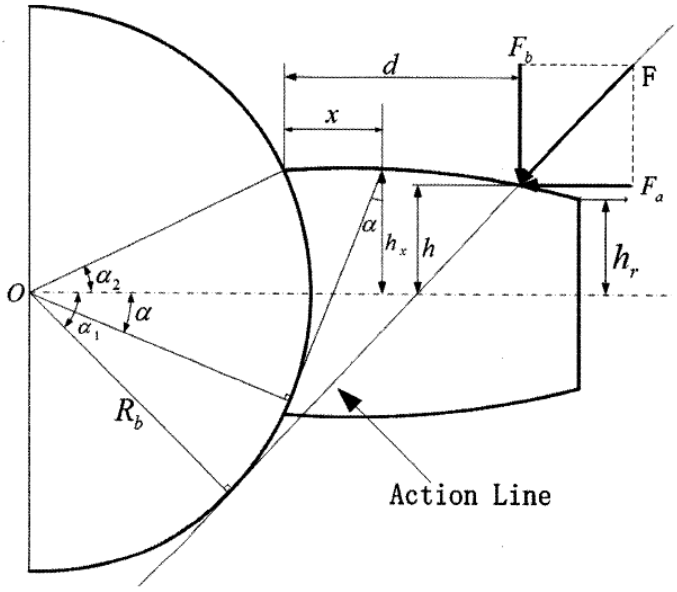

Figure 3.2: Elastic force on gear tooth [10]

From the list of parameter, the equations were developed to calculate the gear meshing stiffness. [10]

$$k_t = \frac{1}{{}^1/_{k_h} + {}^1/_{k_{s1}} + {}^1/_{k_{a1}} + {}^1/_{k_{s2}} + {}^1/_{k_{a2}}} \quad (3.1)$$

$$k_h = \frac{EL\pi}{4(1-\nu^2)} \quad (3.2)$$

$$k_s = \frac{F^2}{2Us} \tag{3.3}$$

$$k_a = \frac{F^2}{2Ua} \tag{3.4}$$

$$M = F_b(d - x) - F_a h \tag{3.5}$$

$$x = R_b[\cos\alpha - (\alpha_2 - \alpha)\sin\alpha - \cos\alpha_2] \tag{3.6}$$

$$d = R_b[(\alpha_1 + \alpha_2)\sin\alpha_1 + \cos\alpha_1 - \cos\alpha_2] \tag{3.7}$$

$$h = R_b[(\alpha_1 + \alpha_2)\cos\alpha_1 - \sin\alpha_1] \tag{3.8}$$

$$\alpha_2 = \frac{\pi}{2N} + \tan\alpha_0 - \alpha_0 \tag{3.9}$$

$$F_a = F\sin\alpha_1 \tag{3.10}$$

$$F_b = F\cos\alpha_1 \tag{3.11}$$

$$U_b = \int_0^d \frac{[F_b(d-x) - F_a h]^2}{2EI_x} dx \tag{3.12}$$

$$U_s = \int_0^d \frac{[1.2F\cos\alpha_1]^2}{2GA_x} dx \tag{3.13}$$

$$I_x = \frac{1}{12}(2h_x)^3 L = \frac{2}{3}h_x^3 \tag{3.14}$$

$$A_x = 2R_b[(\alpha_1 + \alpha_2)\cos\alpha_1 - \sin\alpha_1]L \tag{3.15}$$

$$G = \frac{E}{2(1+\nu)} \tag{3.16}$$

$$\frac{1}{k_s} = \int_{-\alpha_1}^{\alpha_2} \frac{1.2(1+\nu)(\alpha_2-\alpha)\cos\alpha(\cos\alpha_1)^2}{EL[\sin\alpha + (\alpha_2-\alpha)cos\alpha]} d\alpha \tag{3.17}$$

$$\frac{1}{k_a} = \int_{-\alpha_1}^{\alpha_2} \frac{(\alpha_2-\alpha)\cos\alpha(\sin\alpha_1)^2}{2L[\sin\alpha + (\alpha_2-\alpha)cos\alpha]} d\alpha \tag{3.18}$$

During meshing period, the number of pairs of meshing teeth alternates between one and two. During the single tooth meshing, the effective meshing stiffness was calculated by

using Equation (3.1). For double tooth pair meshing duration, the total effective mesh stiffness is shown as in thesis written by Wu [10]

$$k_t = \sum_{i=1}^{2} \frac{1}{1/k_{h,i} + 1/k_{s1,1} + 1/k_{a1,i} + 1/k_{s2,i} + 1/k_{a2,i}} \tag{3.19}$$

Wu [10] also study and derived the calculation expression of mesh stiffness for the single and double tooth pair meshing durations. For this project, the system was assumed by starting with initial double point pair meshing point. The duration could be represented asθ_d. For the single tooth pair meshing point, it was represented asθ_s. Both of the periods were formulated as below:

$$\theta_d = \tan(\arccos\frac{N_1 \cos\alpha_0}{N_1+2}) - \frac{2\pi}{N_1} - tan\Delta \tag{3.20}$$

$$\Delta = \arccos\frac{N_1 \cos\alpha_0}{\sqrt{(N_2+2)^2+(N_1+N_2)^2-2(N_2+2)(N_1+N_2)\cos(\arccos\frac{N_1\cos\alpha_0}{N_1+2}-\alpha_0)}} \tag{3.21}$$

$$\theta_s = \frac{2\pi}{N_1} - \theta_d \tag{3.22}$$

All the equations will be solved by using MATLAB software and Microsoft EXCEL. The previous result obtained by Wu [10], is shown in Figure 3.3.

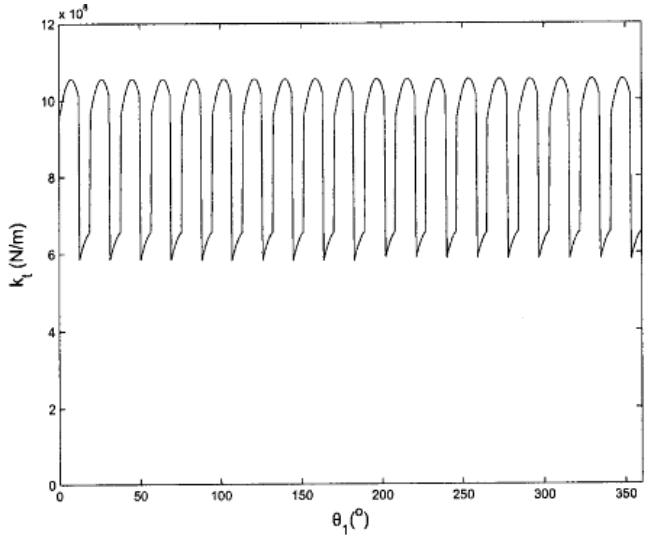

Figure 3.3: Example of result of the total effective mesh stiffness, k_t vs the pinion's angular displacement, θ_1, within one shaft period by.[10]

The calculation for all the equation by using Microsoft EXCEL also provided to observe the result.

3.4 Double/Single-tooth-pair meshing duration.

Based on the equations (3.20) and (3.22) purposed by Wu [10], θ_d andθ_s were referred to double and single meshing gear duration. This is very important in order to estimate when the single and double tooth meshing occur in order to determine the meshing stiffness and plot meshing stiffness graph. In this section, the methodology on how to determine the duration is discussed in detail.

3.4.1 Meshing Stiffness and Calculation for Single and Double Meshing

Axial stiffness (k_a), Hertzian contact stiffness (k_h), Shear stiffness (k_s) and Bending stiffness (k_b) based on equation (3.1) could be calculated for each pair of meshing teeth.

$$k_t = \frac{1}{{}^1\!/_{k_h} + {}^1\!/_{k_{s1,i}} + {}^1\!/_{k_{b1,i}} + {}^1\!/_{k_{a1,i}} + {}^1\!/_{k_{s2,i}} + {}^1\!/_{k_{a2,i}} + {}^1\!/_{k_{b2,i}}}, \qquad i = 1,2 \tag{3.23}$$

The equation (3.23) above is the total meshing stiffness for single and double pair meshing. $k_{s1,i}$, $k_{b1,i}$ and $k_{a1,i}$ are the stiffness at pinion while $k_{s2,i}$, $k_{b2,i}$ and $k_{a2,i}$ are the stiffness at gear. Each of the stiffness can be formulated as equations below:

For pinion spur gear (driving gear)

$$\frac{1}{k_{b1,i}} = \int_{-\alpha_{1,i}}^{\alpha_2} \frac{3\{1+\cos(\alpha_{1,i})[(\alpha_2-\alpha)\sin\alpha-\cos\alpha]\}^2(\alpha_2-\alpha)cos\alpha}{2EL[\sin\alpha+(\alpha_2-\alpha)cos\alpha]^3}\,d\alpha \tag{3.24}$$

$$\frac{1}{k_{s1,i}} = \int_{-\alpha_{1,i}}^{\alpha_2} \frac{1.2(1+\nu)(\alpha_2-\alpha)\cos\alpha(\cos\alpha_{1,i})^2}{EL[\sin\alpha+(\alpha_2-\alpha)cos\alpha]}\,d\alpha \tag{3.25}$$

$$\frac{1}{k_{a1,i}} = \int_{-\alpha_{1,i}}^{\alpha_2} \frac{(\alpha_2-\alpha)\cos\alpha(\sin\alpha_{1,i})^2}{2L[\sin\alpha+(\alpha_2-\alpha)cos\alpha]}\,d\alpha \tag{3.26}$$

For driven gear

$$\frac{1}{k_{b2,i}} = \int_{-\alpha_{1.i}^{'}}^{\alpha_2^{'}} \frac{3\{1+\cos(\alpha_{1,i})[(\alpha_2^{'}-\alpha)\sin\alpha-\cos\alpha]\}^2(\alpha_2^{'}-\alpha)cos\alpha}{2EL[\sin\alpha+(\alpha_2^{'}-\alpha)cos\alpha]^3}\,d\alpha \tag{3.27}$$

$$\frac{1}{k_{s2,i}} = \int_{-\alpha_{1.i}^{'}}^{\alpha_2^{'}} \frac{1.2(1+\nu)(\alpha_2^{'}-\alpha)\cos\alpha(\cos\alpha_{1.i}^{'})^2}{EL[\sin\alpha+(\alpha_2^{'}-\alpha)cos\alpha]}\,d\alpha \tag{3.28}$$

$$\frac{1}{k_{a2,i}} = \int_{-\alpha_{1.i}^{'}}^{\alpha_2^{'}} \frac{(\alpha_2^{'}-\alpha)\cos\alpha(\sin\alpha_{1.i}^{'})^2}{2L[\sin\alpha+(\alpha_2^{'}-\alpha)cos\alpha]}\,d\alpha \tag{3.29}$$

In these equation, i = 1 refer to first pair of meshing teeth while i =2 refer to second pair of meshing teeth. For the angle of α_2 and $\alpha_2^{'}$ are the base circles of pinion and driven gear. Both of the value can be obtained by the formula that has been shown in Table 3.3.

$$\alpha_2 = \left[\frac{\pi}{2N1} + \tan\alpha_0 - \alpha_0\left(\frac{\pi}{180}\right)\right]\left(\frac{180}{\pi}\right) \tag{3.30}$$

$$\alpha_2^{'} = \left[\frac{\pi}{2N2} + \tan\alpha_0 - \alpha_0\left(\frac{\pi}{180}\right)\right]\left(\frac{180}{\pi}\right) \tag{3.31}$$

The value of $\alpha_{1,1}$ (corresponding to α_1 of the pinion) and $\alpha_{1.1}^{'}$ (corresponding to α_1 of the gear) have to be determined in order to calculate all the stiffness.

$$\alpha_{1,1} = \left\{\theta_1 - \frac{\pi}{2N1} + \tan\alpha_0 - \alpha_0\left(\frac{\pi}{180}\right) + \tan\left[\arccos\frac{N_1\cos\alpha_0}{\sqrt{(N_2+2)^2+(N_1+N_2)^2-2(N_2+2)(N_1+N_2)\cos(\arccos\frac{N_1\cos\alpha_0}{N_1+2}-\alpha_0)}}\right]\right\}\left(\frac{180}{\pi}\right)$$

$$\alpha_{1.1}^{'} = \left\{\tan(\arccos\frac{N_2\cos\alpha_0}{N_2+2}) - \frac{\pi}{2N_2} - \left(tan\alpha_0 - \alpha_0\left(\frac{\pi}{180}\right)\right) - \frac{N_1}{N_2}\theta_1\right\}\left(\frac{180}{\pi}\right) \tag{3.33}$$

The equations (3.32) and (3.33) represent the calculation of the angles $\alpha_{1,1}$ and $\alpha_{1.1}^{'}$ respectively which occur at first pair of meshing teeth. This alternately switch with second pair of meshing which corresponding to angles $\alpha_{1,2}$and $\alpha_{1,2}^{'}$. The formulae for both of equations can be expressed as below:

$$\alpha_{1,2} = \left\{\theta_1 + \frac{3\pi}{2N1} + \tan\alpha_0 - \alpha_0\left(\frac{\pi}{180}\right) + \tan\left[\arccos\frac{N_1\cos\alpha_0}{\sqrt{(N_2+2)^2+(N_1+N_2)^2-2(N_2+2)(N_1+N_2)\cos(\arccos\frac{N_1\cos\alpha_0}{N_1+2}-\alpha_0)}}\right]\right\}\left(\frac{180}{\pi}\right)$$

$$\alpha_{1.2}^{'} = \left\{\tan(\arccos\frac{N_2\cos\alpha_0}{N_2+2}) - \frac{N_1}{N_2}\theta_1 - \frac{5\pi}{2N_2} - (tan\alpha_0 - \alpha_0\left(\frac{\pi}{180}\right))\right\}\left(\frac{180}{\pi}\right) \tag{3.35}$$

Based on the equations (3.34) and (3.35), the difference between angle $\alpha'_{1.1}$ and $\alpha'_{1,2}$ is $2\pi/N_2$.

During double tooth pair meshing duration, two pairs of teeth meshing at the same time. This result of increasing of total meshing stiffness which is double from the single tooth pair meshing stiffness that can be calculated based on equation (3.23). For double tooth pair meshing total stiffness can be calculated using the equation of:

$$k_t = \sum_{i=1}^{2} \frac{1}{1/k_h + 1/k_{s1,i} + 1/k_{b1,i} + 1/k_{a1,i} + 1/k_{s2,i} + 1/k_{a2,i} + 1/k_{b2,i}} \quad (3.36)$$

3.5 Calculation of Pinion Meshing Stiffness with Crack Defect

In the section of 3.4, the meshing duration for single and double pair of teeth. This was important to estimate the single or double meshing during the gear rotation. Based on this calculation, the total meshing graph versus angle could be plotted.

In this section, the tooth with crack defect could be detected by calculating the gear tooth meshing stiffness. Basically, the formulae of normal meshing stiffness for single and double pair have been presented in equations (3.23) and (3.36). When crack start to propagate, the total meshing stiffness was changed due the changing amount of shear stiffness (k_s) and bending stiffness. Tian [9] State that the crack usually exists at the root of the pinion and the depth of crack is propagating constantly along the width of tooth and it is represented by 'q' in Figure 3.4.

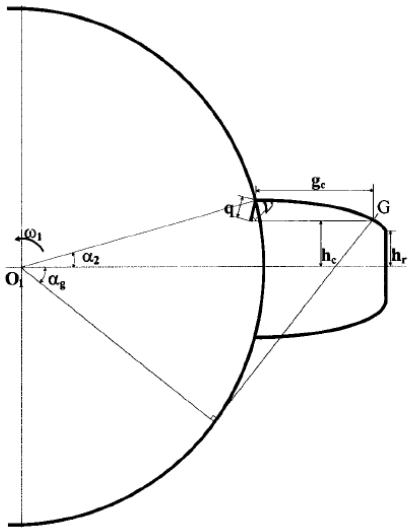

Figure 3.4: A crack tooth [9]

In this study, we followed the (Wu, 2007) methodology which considered the value of q in four conditions which were$h_{c1} \geq h_r \,\&\alpha_1 > \alpha_g$, $h_{c1} \geq h_r \,\&\alpha_1 < \alpha_g$, $h_{c2} \geq h_r \,\&\alpha_1 < \alpha_g$ and $h_{c2} \geq h_r \,\&\alpha_1 > \alpha_g$. Based on mechanical analysis, the value of axial stiffness and Hertzian stiffness remain unchanged during the crack propagation process because the tooth's root crack will not influence the section's strength in bearing axial compressive force and the formulae for both stiffnesses remain the same as in equation (3.2) and (3.18).

3.5.1 Case 1: $\boldsymbol{h_{c1} \geq h_r \,\&\alpha_1 > \alpha_g}$[10]

The crack defect would start to propagate at tooth's root where the stress concentration was highest during meshing period. This could be described in the Figure 3.5.

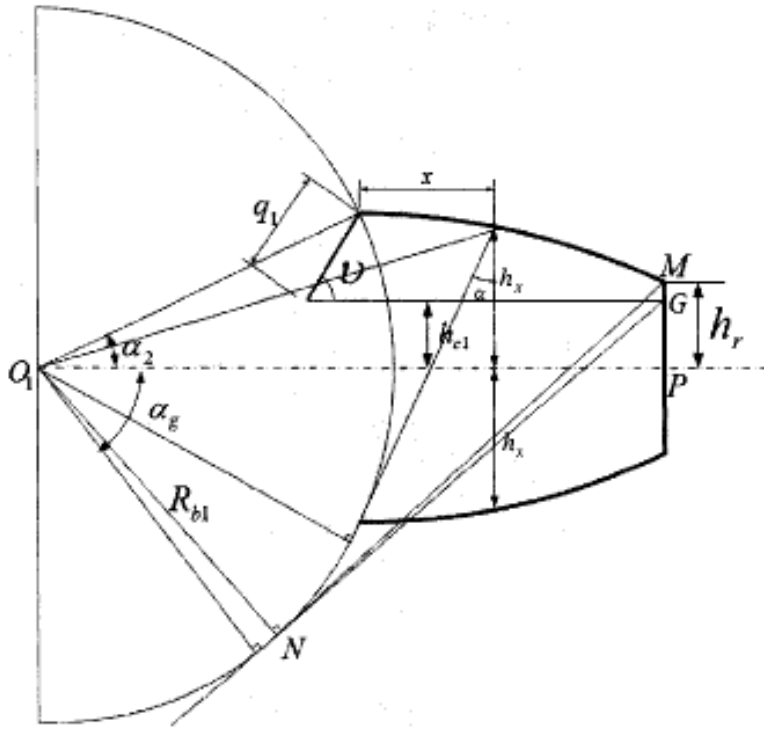

Figure 3.5: Cracked tooth for first case [10]

When the crack start to propagate, the value of h_{c1} would be higher than h_r and it would change the effective area moment of inertia and area of the cross section at distance of x from the tooth root would be calculated as in equations (3.37) and (3.38).

$$I_{xc} = \begin{cases} \frac{1}{12}(h_{c1} + h_x)^3 L, & if\ x \le g_c \\ \frac{1}{12}(2h_x)^3 L, & if\ x > g_c \end{cases} \quad (3.37)$$

$$A_{xc} = \begin{cases} (h_{c1} + h_x)L, & if\ x \le g_c \\ (2h_x)L, & if\ x > g_c \end{cases} \quad (3.38)$$

The value of h_{c1} could be calculated using the equation (3.39) as stated by (Tian, 2004).

$$h_{c1} = R_{b1} sin(\alpha_2) - q \sin(v) \quad (3.39)$$

For this case, the value of x will be higher thang_c, Equation (3.39) was substituted in equation (3.37) and (3.38).The results of substitution as follow:

$$I_{xc} = \frac{1}{12}\{R_{b1}[sin(\alpha_2) + (\alpha + \alpha_2)cos\alpha - sin\alpha] - q_1 \sin(v)\}^3 L \quad (3.40)$$

$$A_{xc} = \{R_{b1}[sin(\alpha_2) + (\alpha + \alpha_2)cos\alpha - sin\alpha] - q_1 \sin(v)\}L \quad (3.41)$$

After the equations (3.40) and (3.41) were obtained, both of these equations then will be replaced into equation (3.12) and (3.13). After further simplification, the equation to calculate bending mesh stiffness for case one becomes:

$$\frac{1}{k_{b(crack)}} = \int_{g}^{\alpha_2} \frac{12\{1+\cos(\alpha_1)[(\alpha_2-\alpha)\sin\alpha-\cos\alpha]\}^2(\alpha_2-\alpha)cos\alpha}{EL\left[\sin\alpha_2-\frac{q_1}{R_{b1}}\sin(v)+\sin\alpha+(\alpha_2-\alpha)cos\alpha\right]^3} d\alpha + \int_{-\alpha_1}^{\alpha_g} \frac{3\{1+\cos(\alpha_1)[(\alpha_2-\alpha)\sin\alpha-\cos\alpha]\}^2(\alpha_2-\alpha)cos\alpha}{2EL[\sin\alpha+(\alpha_2-\alpha)cos\alpha]^3} d\alpha \quad (3.42)$$

The shear mesh stiffness with crack defect could be calculated using equation as obtained below:

$$\frac{1}{k_{s(crack)}} = \int_{-\alpha_g}^{\alpha_2} \frac{2.4(1+\nu)(\alpha_2-\alpha)\cos\alpha(\cos\alpha_1)^2}{EL\left[\sin\alpha_2-\frac{q_1}{R_{b1}}\sin(v)+\sin\alpha+(\alpha_2-\alpha)cos\alpha\right]} d\alpha + \int_{-\alpha_{1,i}}^{\alpha_2} \frac{1.2(1+\nu)(\alpha_2-\alpha)\cos\alpha(\cos\alpha_1)^2}{EL[\sin\alpha+(\alpha_2-\alpha)cos\alpha]} d\alpha \quad (3.43)$$

3.5.2Case 2: $h_{c1} < h_r$ &$\alpha_1 < \alpha_g$ [10]

In case 2, we would calculate the bending mesh stiffness and shear mesh stiffness by assuming the q would be higher than in case 1. This could be described as in Figure 3.6:

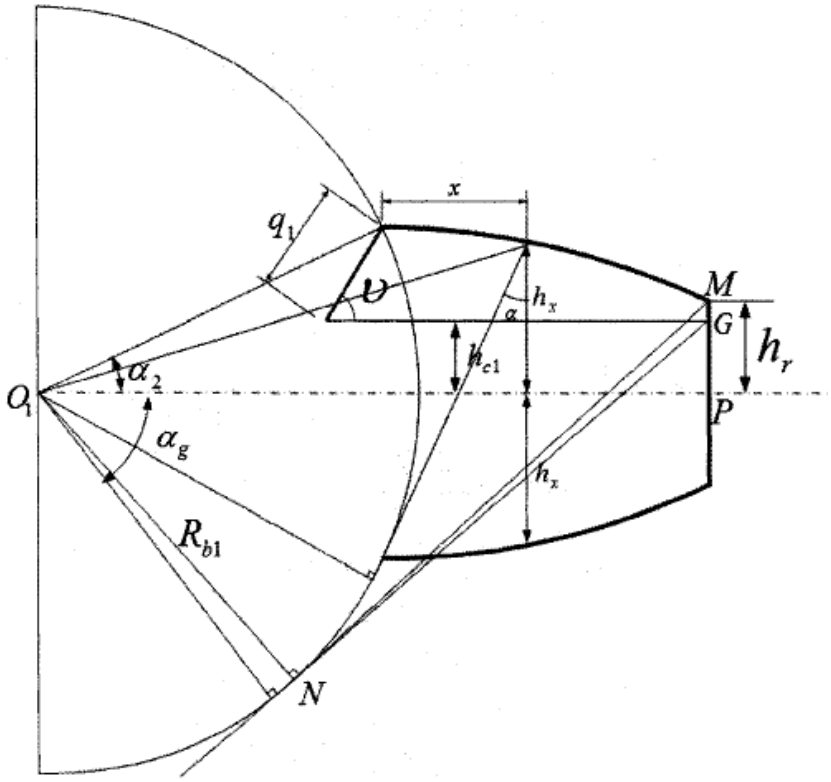

Figure 3.6: Cracked tooth for second case [10]

Area of cross section at the distance x was calculated by using equation (3.44) and (3.45).

$$I_{xc} = \frac{1}{12}\{R_{b1}[sin(\alpha_2) + (\alpha + \alpha_2)cos\alpha - sin\alpha] - q_2 \sin(v)\}^3 L \quad (3.44)$$

$$A_{xc} = \{R_{b1}[sin(\alpha_2) + (\alpha + \alpha_2)cos\alpha - sin\alpha] - q_2 \sin(v)\} L \quad (3.45)$$

The equation then would be substituted into equation (3.12) and (3.13) respectively. The value of shear mesh stiffness and bending mesh stiffness for second could be calculated using equation (3.46) and (3.47).

$$\frac{1}{k_{b(crack)}} = \int_{-\alpha_1}^{\alpha_2} \frac{12\{1+\cos(\alpha_1)[(\alpha_2-\alpha)\sin\alpha-\cos\alpha]\}^2(\alpha_2-\alpha)cos\alpha}{EL\left[\sin\alpha_2-\frac{q_2}{R_{b1}}\sin(v)+\sin\alpha+(\alpha_2-\alpha)cos\alpha\right]^3} d\alpha \quad (3.46)$$

$$\frac{1}{k_{s(crack)}} = \int_{-\alpha_1}^{\alpha_2} \frac{2.4(1+\nu)(\alpha_2-\alpha)\cos\alpha(\cos\alpha_1)^2}{EL\left[\sin\alpha_2-\frac{q_2}{R_{b1}}\sin(v)+\sin\alpha+(\alpha_2-\alpha)cos\alpha\right]} d\alpha \quad (3.47)$$

The crack in second case would continuously propagate until it reached the tooth's central line and then the direction of the crack propagation would change and would be discussed in case 3.

3.5.3Case 3: $h_{c2} \geq h_r$ &$\alpha_1 < \alpha_g$[10]

Case 3 was similar to case 1 but the direction of the crack propagation was changing. It could be described as in Figure 3.7:

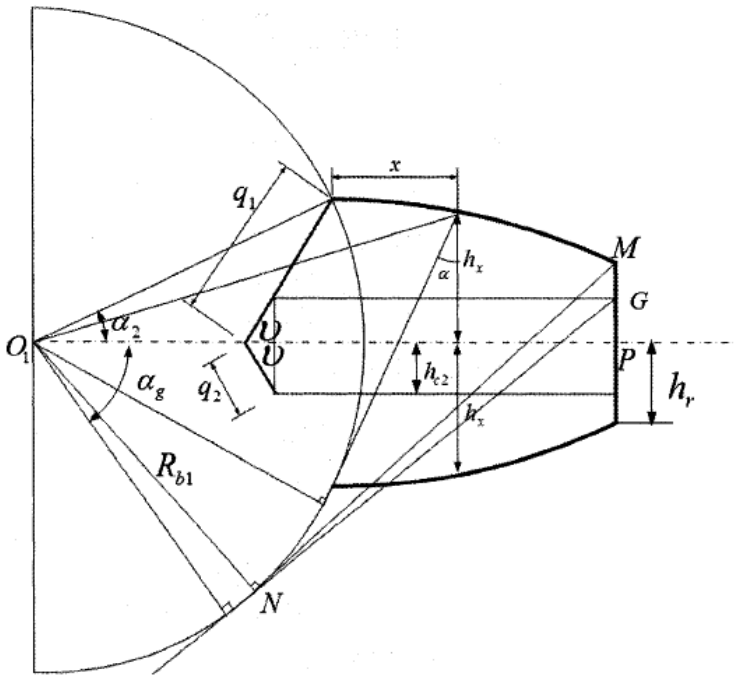

Figure 3.7: Cracked tooth for third case [10]

The value of I_{xc} and A_{xc} were calculated using equation (3.44) and (3.45) but using different value of q. Then, the shear mesh stiffness and bending mesh stiffness were calculated using the following equations:

$$\frac{1}{k_{b(crack)}} = \int_{-\alpha_g}^{\alpha_2} \frac{12\{1+\cos(\alpha_1)[(\alpha_2-\alpha)\sin\alpha-\cos\alpha]\}^2(\alpha_2-\alpha)cos\alpha}{EL\left[\sin\alpha-\frac{q_3}{R_{b1}}\sin(v)+(\alpha_2-\alpha)cos\alpha\right]^3}d\alpha \qquad (3.48)$$

$$\frac{1}{k_{s(crack)}} = \int_{-\alpha_g}^{\alpha_2} \frac{2.4(1+\nu)(\alpha_2-\alpha)\cos\alpha(\cos\alpha_1)^2}{EL\left[\sin\alpha-\frac{q_3}{R_{b1}}\sin(v)+(\alpha_2-\alpha)cos\alpha\right]} d\alpha \quad (3.49)$$

3.5.4Case 4: $h_{c2} \geq h_r$ &$\alpha_1 > \alpha_g$[10]

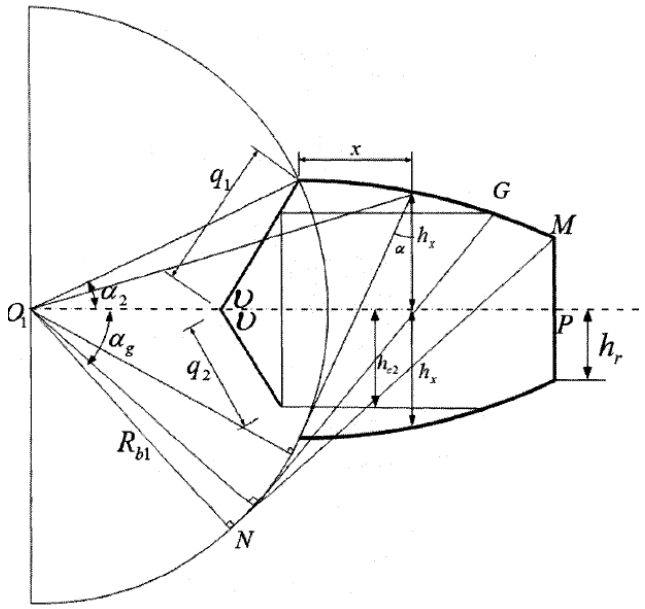

Figure 3.8: Cracked tooth for fourth case [10]

Figure 3.8 represents the schematic diagram of a crack before reaching the end of tooth point. The method of calculating the shear mesh stiffness and bending mesh stiffness was same as in first until third case. But the equations were changed due to different value of q as stated in the equations 3.50 and 3.51

$$\frac{1}{k_{b(crack)}} = \int_{-\alpha_g}^{\alpha_2} \frac{12\{1+\cos(\alpha_1)[(\alpha_2-\alpha)\sin\alpha-\cos\alpha]\}^2(\alpha_2-\alpha)cos\alpha}{EL\left[\sin\alpha-\frac{q_4}{R_{b1}}\sin(v)+(\alpha_2-\alpha)cos\alpha\right]^3} d\alpha \quad (3.50)$$

$$\frac{1}{k_{s(crack)}} = \int_{-\alpha_g}^{\alpha_2} \frac{2.4(1+\nu)(\alpha_2-\alpha)\cos\alpha(\cos\alpha_1)^2}{EL\left[\sin\alpha-\frac{q_4}{R_{b1}}\sin(v)+(\alpha_2-\alpha)cos\alpha\right]} d\alpha \quad (3.51)$$

3.6 Result that Obtained From [10]

In (Wu, 2007), 4 different value of crack length, q have been used in order to determine the value of total mesh stiffness. The values could be referred as in Table 3.3.

Table 3.3: Sample of different crack length (Wu, 2007)

q_1 =1.4 mm	**Case 1**
q_2 = 3.1mm	**Case 2**
q_3 = 1.1 mm (different direction)	**Case 3**
q_4 = 2.4mm (different direction)	**Case 4**

All the result were plotted in graph total meshing stiffness versus angular gear rotation to study the study the response of the gear meshing with crack propagation. All these values would be validated by using the value in experimental data. Table 3.9 shows the result for every crack size that influence the total gear meshing stiffness. For crack with size of 1.4 mm, the meshing stiffness reduced during single and double tooth meshing. The size of crack became bigger to size of 3.1 mm. This was because of the stress that concentrated at the crack point. The total gear meshing stiffness represented by k_t became smaller than the first result. After the crack reached the central line of the tooth, the rack changed the direction. Tian had assumed that the crack changed it direction by 45^o. For case 3, the crack was divided into two parts that effected the total gear meshing. From the graph of case 3 we could see that the crack size from the both parts caused the drastic decrease of meshing stiffness compare to case 1 and case 2. Then, in case 4 where the crack propagated before it reached the end point of gear tooth. The crack size for second part was 2.4 mm. So, the total gear meshing stiffness keep decreasing until it reached the end point. Then it will consider as broken tooth where the total gear stiffness equal to zero because there is no tooth meshing.

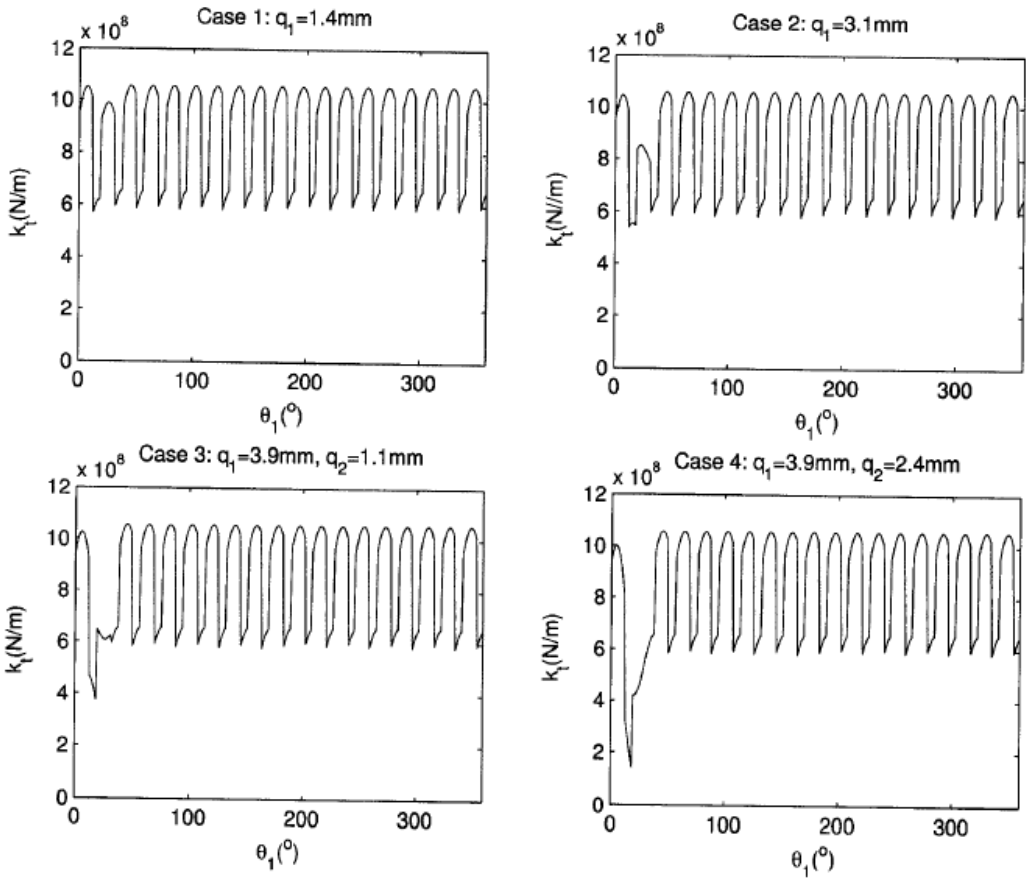

Fig 3.9: The total meshing stiffness at different crack value [10]

CHAPTER 4

RESULT

From the first model, the result for gear meshing stiffness was obtained by solving equation 3.1 until equation 3.22. This was to determine the total mesh stiffness at normal gear as the basic data of the experiment before proceed with the model with crack defect. The parameter that needed to be considered such as Poisson's ratio, young modulus, pressure angle, number of pinion teeth and number of gear teeth and width of teeth. This model was using the same material which is Aluminum 6061. The model was simulated to see the relation between the increasing of contact angle represent by α for the base model without defect. Ten models have been developed with varies contact angle and the results shows the various value of bending stiffness, k_b, shear stiffness, k_s and axial load stiffness, k_a. All the results are shown in Table 4.1.

Based on the data from the first model (Table 4.1) however there were many mistakes that have been done previously including the value of parameters such as the value of α_1, α_2, F, R_{b1} , h and x. This was due to lack of information and data from previous study. The second model was developed with more good result by plotting the graph of total meshing stiffness. But the second model still not good enough to get better result because the meshing period for single and double pair cannot be determined. The result shows the gear meshing is plotting harmonically and not in the form of Fourier series because the unknown value of single and double meshing period. The result can be seen in Table 4.2 and Figure 4.1. Compared to graph that provide by (Wu, 2007), the difference of total meshing stiffness was very high due to different material that was used for this study. [10]

Table 4.1: Result of the calculation using Microsoft EXCEL (first model)

	for alpha=5	for alpha=10	for alpha=15	for alpha=20	for alpha=25	for alpha=30	for alpha=35	for alpha=40	for alpha=	for alpha=50
Material:	Aluminum 6061	Aluminum 6061	Aluminum 6061	Aluminum 6061	Aluminum 6061	Aluminum 6061	Aluminum 6061	Aluminum 6061	Aluminun	Aluminum 6061
Density:	2.7	2.7	2.7	2.7	2.7	2.7	0.7	2.7	2.7	3.7
UTS	310000000	310000000	310000000	310000000	310000000	310000000	310000000	310000000	3.1E+08	310000000
TS	275000000	275000000	275000000	275000000	275000000	275000000	275000000	275000000	2.75E+08	275000000
Modulus of elastic	69000000000	69000000000	69000000000	69000000000	69000000000	69000000000	69000000000	69000000000	6.9E+10	69000000000
Fatigue strength	95000000	95000000	95000000	95000000	95000000	95000000	95000000	95000000	95000000	95000000
Poisson ratio	0.33	0.33	0.33	0.33	0.33	0.33	0.33	0.33	0.33	0.33
Pressure angle	20	20	20	20	20	20	20	20	20	20
N1	19	19	19	19	19	19	19	19	19	19
N2	48	48	48	48	48	48	48	48	48	48
Young modulus	68600000000	68600000000	68600000000	68600000000	68600000000	68600000000	68600000000	68600000000	6.86E+10	68600000000
Shear modulus	26000000000	26000000000	26000000000	26000000000	26000000000	26000000000	26000000000	26000000000	2.6E+10	26000000000
Diameter pitch	0.2032	0.2032	0.2032	0.2032	0.2032	0.2032	0.2032	0.2032	0.2032	0.2032
Width of teeth	0.016	0.016	0.016	0.016	0.016	0.016	0.016	0.016	0.016	0.016
conftact force F	20	20	20	20	20	20	20	20	20	20
Fa	18.25890501	18.25890501	18.25890501	18.25890501	18.25890501	18.25890501	18.25890501	18.25890501	18.25891	18.25890501
Fb	8.161641236	8.161641236	8.161641236	8.161641236	8.161641236	8.161641236	8.161641236	8.161641236	8.161641	8.161641236
Rb	0.5	0.5	0.5	0.5	0.5	0.5	0.5	0.5	0.5	0.5
alpha (1)	5	10	15	20	25	30	35	40	45	50
alpha	12.08616094	12.08616094	12.08616094	12.08616094	12.08616094	12.08616094	12.08616094	12.08616094	12.08616	12.08616094
alpha(2)-2	57.64516094	57.64516094	57.64516094	57.64516094	57.64516094	57.64516094	57.64516094	57.64516094	57.64516	57.64516094
d	14.40704611	14.40704611	14.40704611	14.40704611	14.40704611	14.40704611	14.40704611	14.40704611	14.40705	14.40704611
h	14.45955987	14.45955987	14.45955987	14.45955987	14.45955987	14.45955987	14.45955987	14.45955987	14.45956	14.45955987
x	3.095927924	-0.295527008	0.124124056	3.37304288	-0.802432235	-9.216043064	-5.800949531	9.622566348	13.82246	-4.934785015
M	-171.6984416	-144.0186032	-147.4436446	-173.9601544	-139.8814246	-71.21255147	-99.08531967	-224.9665229	-259.245	-106.1546437
Ix	1.043626268	-31.04104512	-51.01337292	9.638969371	267.7962346	2.231943193	-398.6238024	-238.2718887	131.9365	1162.01737
Ax	0.092889952	-0.287805564	-0.339637071	0.194893463	0.59027614	0.119678128	-0.673971423	-0.567733702	0.466203	0.962774576
G	51578947368	51578947368	51578947368	51578947368	51578947368	51578947368	51578947368	51578947368	5.16E+10	51578947368
Ub	0.0004358	0.0004358	0.0004358	0.0004358	0.0004358	0.0004358	0.0004358	0.0004358	0.000436	0.0004358
Us	1.38238E-07	-3.90385E-07	-2.71175E-07	1.36362E-07	2.65622E-07	3.17276E-08	-1.93372E-07	-1.25032E-07	9.45E-08	1.54345E-07
Ua	4.15796E-07	-4.3193E-08	-5.2297E-08	1.79628E-07	1.24648E-09	3.42616E-07	-1.14261E-08	-4.10753E-08	6.52E-08	3.00331E-09
kb	458926.1129	458926.1129	458926.1129	458926.1129	458926.1129	458926.1129	458926.1129	458926.1129	458926.1	458926.1129
ks	1446777550	-512315062.2	-737531481.7	1466689468	752949913.2	6303651362	-1034275696	-1599593311	2.12E+09	1295795521
ka	481004660.9	-4630382292	-3824309124	1113414763	1.60452E+11	583743777.8	-17503805590	-4869107656	3.07E+09	66593120175
delta	1.107467681	1.107467681	1.107467681	1.107467681	1.107467681	1.107467681	1.107467681	1.107467681	1.107468	1.107467681
Delta d	-6.709755197	-6.709755197	-6.709755197	-6.709755197	-6.709755197	-6.709755197	-6.709755197	-6.709755197	-6.70976	-6.709755197
Delta s	7.040492039	7.040492039	7.040492039	7.040492039	7.040492039	7.040492039	7.040492039	7.040492039	7.040492	7.040492039

Table 4.2: Data for second model

α	0	5	10	15	20	25	30	35	40	45	50
α2	-19.62694977	-19.6269498	-19.6269498	-19.6269498	-19.6269498	-19.6269498	-19.6269498	-19.6269498	-19.6269498	-19.6269498	-19.6269
x	5.105052318	8.62733597	13.54761775	19.8121512	27.34623413	36.05498299	45.82434088	56.52230933	68.00039193	80.0952352	92.63045
d	11.78751103	11.78751103	11.78751103	11.78751103	11.78751103	11.78751103	11.78751103	11.78751103	11.78751103	11.78751103	11.78751
h	64.52942522	64.52942522	64.52942522	64.52942522	64.52942522	64.52942522	64.52942522	64.52942522	64.52942522	64.52942522	64.52943
M	-51071.31089	-52377.8719	-54203.0083	-56526.7834	-59321.4869	-62551.9228	-66175.7825	-70144.1024	-74401.7989	-78888.2775	-83538.1
Ix	-4737.999688	-1973.78602	-563.900738	-66.2364362	3.82696E-07	55.10498452	382.5355478	1087.903039	2099.227409	3206.842776	4133.947
G	25939849624	25939849624	25939849624	25939849624	25939849624	25939849624	25939849624	25939849624	25939849624	25939849624	2.59E+10
Ax	1.290588504	1.290588504	1.290588504	1.290588504	1.290588504	1.290588504	1.290588504	1.290588504	1.290588504	1.290588504	1.290589
Us	1.09282E-05	1.09282E-05	1.09282E-05	1.09282E-05	1.09282E-05	1.09282E-05	1.09282E-05	1.09282E-05	1.09282E-05	1.09282E-05	1.09E-05
Ua	4.55785E-05	4.55785E-05	4.55785E-05	4.55785E-05	4.55785E-05	4.55785E-05	4.55785E-05	4.55785E-05	4.55785E-05	4.55785E-05	4.56E-05
ks	37804066252	37804066252	37804066252	37804066252	37804066252	37804066252	37804066252	37804066252	37804066252	37804066252	3.78E+10
ka	9064112847	9064112847	9064112847	9064112847	9064112847	9064112847	9064112847	9064112847	9064112847	9064112847	9.06E+09
kh	608231399.4	608231399.4	608231399.4	608231399.4	608231399.4	608231399.4	608231399.4	608231399.4	608231399.4	608231399.4	6.08E+08
kt	561517472.9	280758736.5	561517472.9	280758736.5	561517472.9	280758736.5	561517472.9	280758736.5	561517472.9	280758736.5	5.62E+08

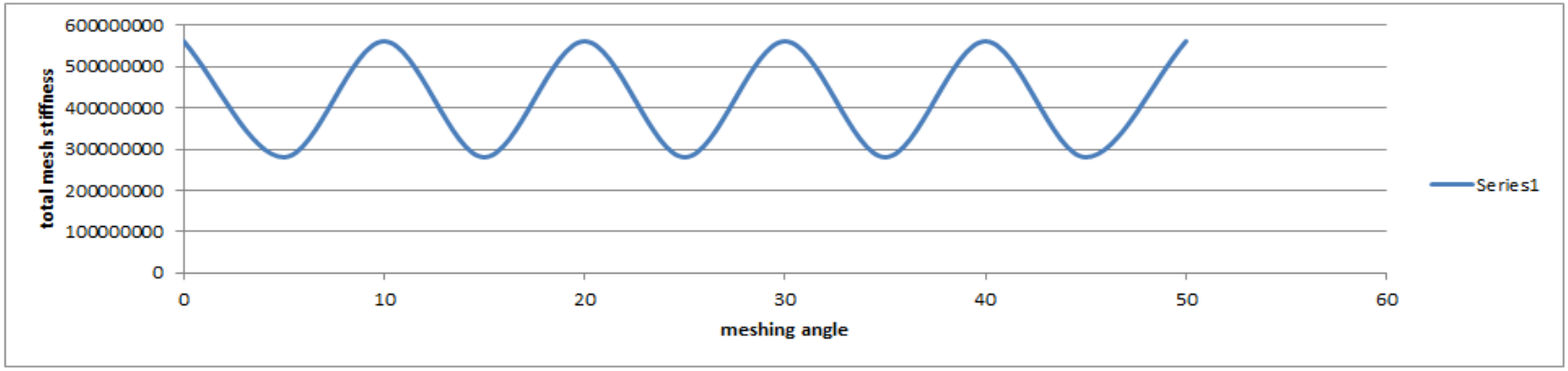

Figure 4.1: The pattern of total meshing stiffness

4.1 Comparison of Result (Third Model)

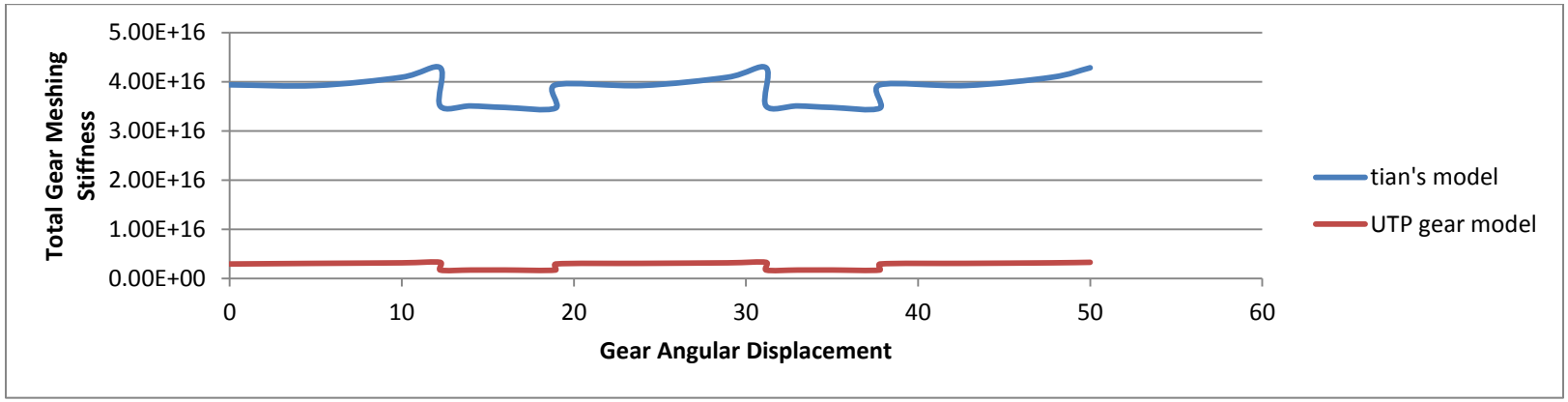

Figure 4.2(a): The comparison between Tian's model and experimental model (same number of tooth)

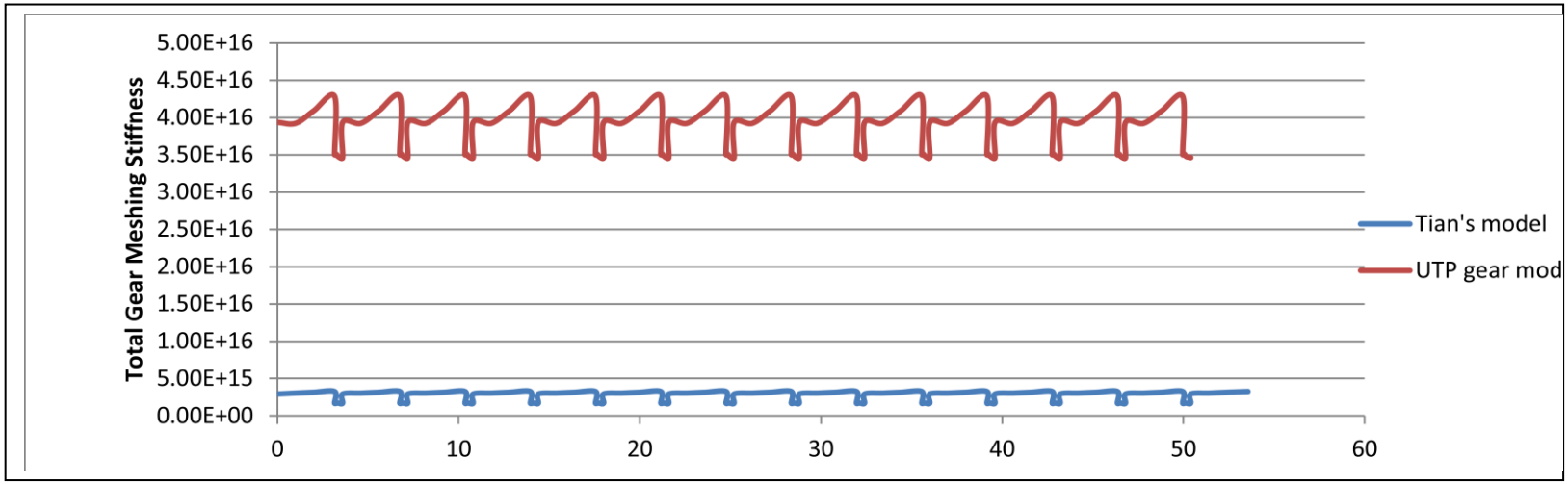

Figure 4.2(b): The comparison between Tian's model and experimental model (same material)

The study proceeds with the third model where the meshing period for single and double are calculated. Figure 4.2(a) and Figure 4.2(b) show the comparison between Tian's model and UTP gear model. The different between these two models was based on the total gear meshing stiffness and period during single and double meshing period. For Tian's model, the total meshing stiffness for single and double meshing was higher than experimental model because Tian's model uses mild steel in order to model the gear meanwhile the experimental model uses Aluminum S6061. The value of young modulus affects the total gear meshing stiffness. The value of Young Modulus for mild steel is 2.068×10^{11} Pa and the value of Young Modulus for Aluminum S6061 is 6.9×10^{10}. These two different values was effecting the result of total gear meshing stiffness because the equation for axial stiffness, Hertzian contact stiffness, shear stiffness and bending stiffness involving the value of Young Modulus represented by capital E. The other different between these two models was the period for single and double gears meshing. The period of gear meshing depends on the number of tooth of pinion and gear. If the number of teeth is higher, the period for gear meshing will be shorter. This could be verified based on the equation 3.20 and equation 3.22. For Tian's model, the period for double gear meshing is 12.232 seconds and for double gear is 6.704 seconds. For the experimental model the period for double gear meshing is 3.157 seconds and for single gear meshing is 0.443 seconds. All of these values were represented in Table (4.3) until Table (4.6). So, we could conclude that number of teeth effects the gear meshing period.

From Figure 4.3a until Figure 4.3d show the results of gear simulation for the mathematical gear model with various crack size. The crack size in Figure 4.3a was estimated as 0.0014m. This was the state where the crack started to propagate. The propagation of crack caused the total gear meshing stiffness to drop or decreased drastically. This was due to changing of value from the summation of the total meshing stiffness. When the crack started to propagate, the value of bending and shear stiffness change. The value for Hertzian contact stiffness remained the same due to unchanged in parameter in equation 3.2. For the axial stiffness, the value also remains unchanged due to the crack defect because crack will not influence the section's strength in bearing axial

compressive force. We could see how the size of the crack effecting the total meshing stiffness. If the crack size was bigger or longer, the total meshing stiffness would lesser. When the crack reach the center line of gear tooth, the direction of the crack would change symmetrically and the assumption that could be made for this mathematical model was the crack would change its direction by 45^{o}. As the crack become larger, the total meshing stiffness become smaller.

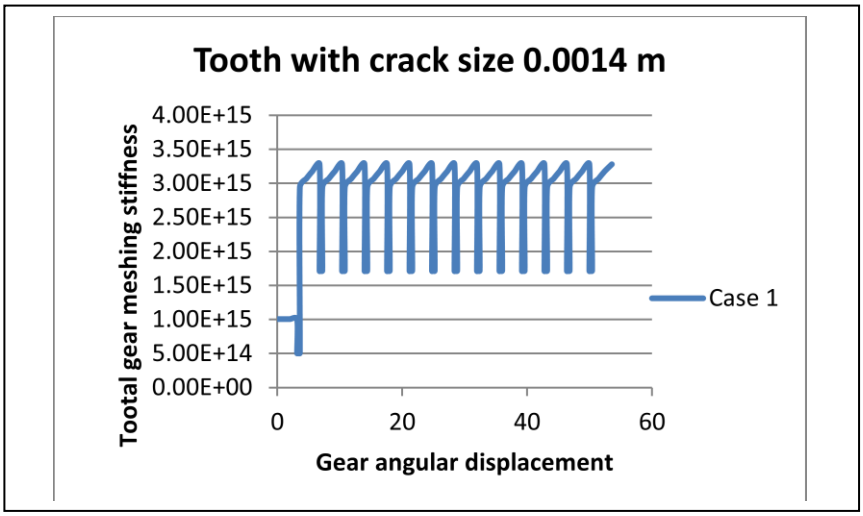

Figure 4.3a: Gear with 0.0014 crack

In Figure 4.3b, the length of the crack was 0.003 m. This can be compared to case 2 of Tian's model [9] but with different crack size. The total gear meshing for single and double tooth meshing were lower than first case where the size of crack is 0.003 m.

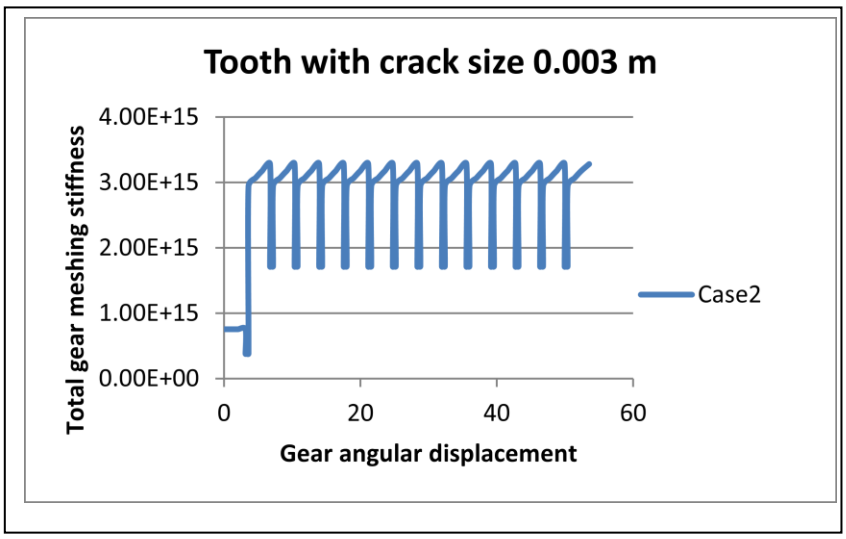

Figure 4.3b: Gear with 0.003 crack

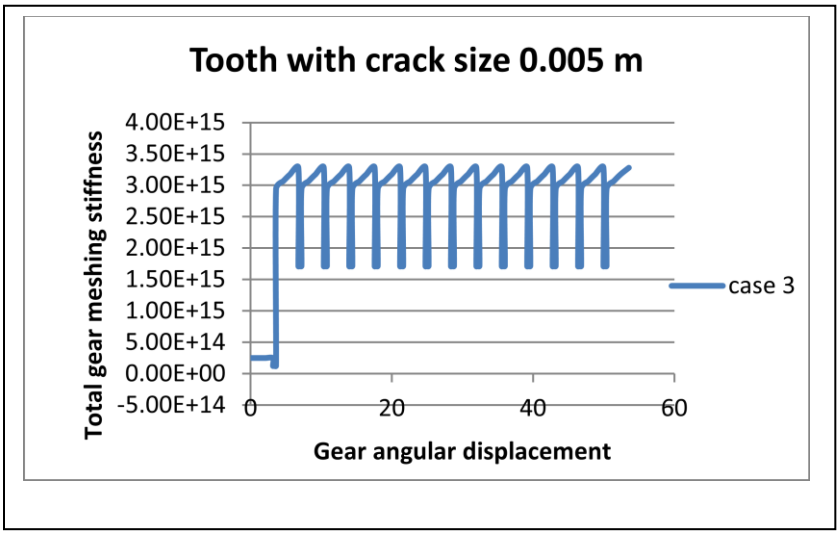

Figure 4.3c: Gear with 0.005 crack

The crack would propagate until it reached the end point of the tooth and the tooth would totally brake. At this stage, the total gear meshing could be considered as zero because there was no meshing between tooth of pinion and tooth of gear. As in Figure 4.3d, the result showed that the total meshing stiffness drop to zero during single meshing because as mentioned before the meshing of broken tooth of pinion and tooth of gear was not happened. Using MATLAB did all the calculations of the total meshing stiffness and the coding was shown in section 4.2.

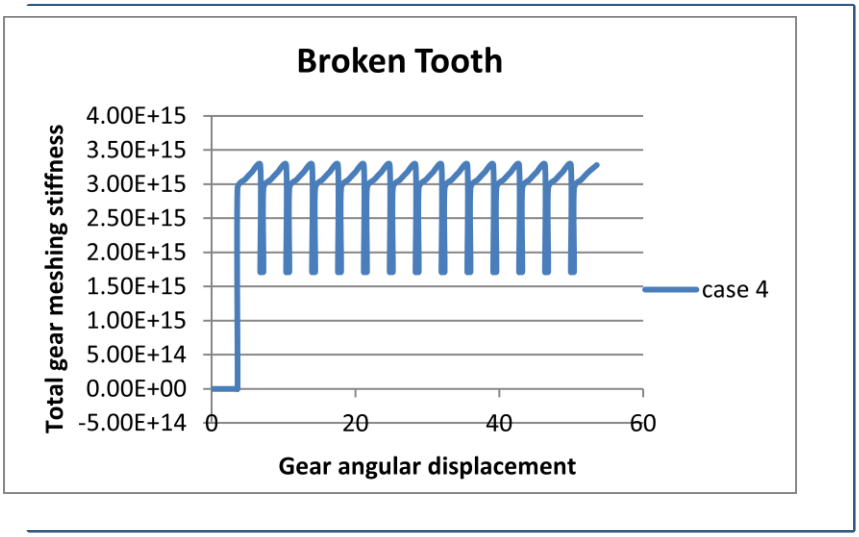

Figure 4.3d: Gear with broken tooth

Table 4.3 until 4.6 shows the data for Tian´s model include angular displacement during single and double gear meshing, $\alpha_{1,1}$, $\alpha_{1,2}$, α_2, bending stiffness (k_b), Shear stiffness (k_s), Hertzian contact stiffness and total meshing gear stiffness. As mentioned before all the result was obtained from solving the equation 3.2 until equation 3.19. This was to obtain the result for Tian's model. For single pair of pinion, it happened during single pair of tooth meshing. By solving equation 3.22, the value of θ_s could be obtained. Θ_d could be obtained by solving equation 3.20. The values of $\alpha_{1,1}$ also could be obtained by solving equation 3.32. $\alpha_{1,2}$ is the value for tooth during double pair gear meshing and it could be calculated by using equation 3.34. α_2 is half tooth angle and it occurs at both pinion and gear. This value could be obtained by solving equation 3.9.

Table 4.3: Single Pair for Pinion Meshing Data (Tian's model)

theta	$\alpha_{1,1}$	α_2	(1/kb)	(1/ks)	(1/ka)	(1/kh)	1/kt
0	-1.2396	5.591	6.38E+12	6.48E-08	1.41E-09	2.86E+09	6.38E+12
5	3.7604		2.79E+14	1.44E-07	3.14E-09	2.86E+09	2.79E+14
10	8.7604		2.27E+15	2.24E-07	4.88E-09	2.86E+09	2.27E+15
12.232	10.9924		4.34E+15	2.60E-07	5.65E-09	2.86E+09	4.34E+15

Table 4.4: Single Pair for Gear Meshing Data (Tian's model)

theta	$\alpha_{1,1}'$	$\alpha_{2'}$	(1/kb)	(1/ks)	(1/ka)	(1/kh)	1/kt
0	24.659	2.729	4.02E+15	4.44E-07	3.99E-07	2.86E+09	4.02E+15
5	22.814		3.87E+15	4.14E-07	3.72E-07	2.86E+09	3.87E+15
10	20.969		3.87E+15	3.84E-07	3.45E-07	2.86E+09	3.87E+15
12.232	20.145392		3.86E+15	3.71E-07	3.33E-07	2.86E+09	3.86E+15

Table 4.5: Double Pair for Pinion Meshing Data (Tian's model)

theta	$\alpha_{1,2}$	α_2	(1/kb)	(1/ks)	(1/ka)	(1/kh)	1/kt
12.232	29.886	5.591	3.34E+16	5.63E-07	1.22E-08	2.86E+09	3.34E+16
14	31.654		3.34E+16	5.91E-07	1.29E-08	2.86E+09	3.34E+16
16	33.654		3.34E+16	6.23E-07	1.35E-08	2.86E+09	3.34E+16
18.936	36.59		3.37E+16	6.70E-07	1.46E-08	2.86E+09	3.37E+16

Table 4.6: Double Pair for Gear Meshing Data (Tian's model)

theta	$\alpha_{1,2}'$	$\alpha_{2'}$	(1/kb)	(1/ks)	(1/ka)	(1/kh)	1/kt
12.232	12.2955744	2.729	1.96E+15	2.43E-07	2.18E-07	2.86E+09	1.96E+15
14	11.5958		1.66E+15	2.32E-07	2.07E-07	2.86E+09	1.66E+15
16	10.8042		1.33E+15	2.19E-07	1.96E-07	2.86E+09	1.33E+15
18.936	9.6421312		9.24E+14	2.00E-07	1.79E-07	2.86E+09	9.24E+14

4.2 MATLAB Coding

To solve the complex of integration of meshing stiffness like equation (3.27), (3.28) and (3.29), calculator cannot be used to obtain the result. The powerful software such as MATLAB was used to calculate the result precisely. The method that used to solve complex integration equation to calculate meshing stiffness was called **adaptive Simpson quadrature.**

4.2.1 Total Mesh Stiffness for Normal Gera and Pinion (MATLAB Code)

The equations that have been listed in methodology part were calculated by using MATLAB coding such as Hertzian contact stiffness (eq. 2) axial stiffness for pinion (eq. 3.24), bending stiffness (eq. 3.25), shear stiffness (eq. 3.26), pinion single meshing, pinion double meshing, gear single meshing, gear double meshing and meshing duration. All of these codes are simulated by the main program. All the MATLAB coding could be referred in appendix.

CHAPTER 5

CONCLUSION AND RECOMMENDATION

5.1 CONCLUSION

The major problem of the mathematical gear modeling in this project was to find the right parameter from the previous study. This was because all the articles that have been found did not state the value and came out with the result without detail calculation explanation. The normal gear model then compared to the model that used parameter from experimental method. This was to evaluate the method of meshing calculation from (Wu, 2007) at different crack size. From the first and second mathematical model involving the total mesh stiffness, this model was very useful in order to get the correct value of total gear mesh stiffness. Some of the value might not be unreasonable due to wrong parameter that was used to develop the model. In the third mathematical model of spur gear, the total mesh stiffness like in first until fourth case were developed by using the experimental model data and compared with past study result in order to validate the method. Wu and Tian used the same method. This method was developed by Xianhao Tian and known as Tian's method. The direct calculation of meshing stiffness was based on the total stiffness of Hertzian contact stiffness, shear stiffness, bending stiffness and axial stiffness. All the result was plotted in graph to analyze the meshing characteristic.

5.2 RECOMMENDATION

This model can be improved by developing the force function model in order to determine the rate of crack propagation which can be modeled using the force and torque parameters. Possible future research related to gear defect is listed below:

1. Study of the rate of crack propagation at gear under various loading conditions.
2. Gear meshing characteristic with various gear defects such as tooth wear and pitting.

CHAPTER 6

REFERENCES

[1]Ozguven, H., & Houser, D. (1988). Mathematical models used in gear dynamic. *Journal of Sound and Vibration*, 121.

[2] Parey, A., & N., T. (2003). Spur gear dynamic models including defects. *The Shock and Vibration Digest 35 (6)*, 465-478.

[3] RW, C. (1981). Compliance and stress sensitivity of spur gear teeth. *ASME J. Mech. Des. 103*, 447-459.

[4] Parey, A., Badaoui, M., Guillet, F., & Tandon, N. (2006). Dyanamic modelling of spur gear pair and application of empirical mode decomposition-based statistical analysis for early detection of localized tooth defect. *Journal of soubd and vibration*.

[5] Cj, L., Lee, H., & Choi, S. (2002). Estimating size of gear tooth root crack uses embedded modeling. *Mech Syst Signal Process*, 41-52.

[6] Li, C., & Lee, H. (2005). Gear fatigue crack prognosis using embedded-dynamic-fracture model, gear dynamic model and fracture mechanics. *Mech Syst Signal Process*, 36-46.

[7] Chen, Z., & Siao, Y. (2011). Dynamic simulation of spur gear with tooth crack propogating along tooth width and crack depth. *Engineering Failure Analysis 18 (2011) 2149-264*, 1-15.

[8] Fakher, C., Tahar, F., & Haddar, M. (2009). Analytical modelling of spur gear tooth crack and influence on gearmesh stiffness. *European Journal of Mechanics A/Solids* , 461-468.

[9]Tian, X. (2004). *Dynamic Simulation for System Response of Gearbox Including Localized Gear Faults.* Alberta: University Of Alberta.

[10]Wu, S. (2007). *Gearbox Dynamic Simulation and Estimation of Fault Growth.* Ottawa: ProQuest Dissertations and Thesis.

APPENDIX I

Project Milestone (FYP1)

Important Milestones/Week	1	2	3	4	5	6	7		8	9	10	11	12	13	14
Preliminary Research	■	■	■					MID-SEMESTER BREAK							
Approval of Title Selection				●											
Project work commencement/Completion of extended proposal					■	■									
Submission of extended proposal (FYP 1)						●									
Continuation of project work/preparation for seminar							■		■	■					
Proposal defence/seminar											●				
Fabrication of gear sets											■	■			
Experiment for baseline data												■	■	■	
Submission of Interim Draft Report (FYP 1)														●	
Submission of Interim Report (FYP 1)															●

APPENDIX II

Project Milestone (FYP2)

Important Milestones/Week	1	2	3	4	5	6	7	MID-SEMESTER BREAK	8	9	10	11	12	13	14	15
Experiment for faulty gear sets	■	■	■	■	■	■	■									
Submission of Progress Report									●							
Analysis of vibration data									■	■	■	■	■			
Submission of Draft Report													●			
Submission of Dissertation (Final Draft Report - Soft Bound)														●		
Submission of Technical Paper														●		
Oral Presentation/Viva															●	
Submission of Dissertation (Hard Bound)																●

APPENDIX III

MATHLAB Coding

Axial stiffness for pinion

```
%% Axial Stiffness
functionya = stiff_ka(a)
global E L mu a2v a1v index
if index ==1
    a1 = a1v(1);
    a2 = a2v(1);
elseif index ==2
    a1 = a1v(2);
    a2 = a2v(2);
elseif index ==3;
    a1 = a1v(3);
    a2 = a2v(1);
elseif index ==4
    a1 = a1v(4);
    a2 = a2v(2);
end
caln1 = (a2 - a).*cos(a)*power(sin(a1),2);
caln2 = 2*E*L*power(sin(a) + (a2 - a)*cos(a),1);
ya = caln1./caln2;
```

Bending stiffness for pinion

```
functionyb = stiff_kb(a)
global E L mu a2v a1v index if index ==1
    a1 = a1v(1);
    a2 = a2v(1);
elseif index ==2
    a2 = a2v(2);
end
a
caln1 = 3.*power(1 + cos(a1.*((a2 - a).*sin(a) - cos(a))),2).*(a2 -
a).*cos(a);
caln2 = 2*E*L*power(sin(a) + (a2 - a).*cos(a),3);
yb = caln1./caln2;

y = 3.*caln1.*caln2./2.*(cald1.*cald2);

%%
```

Shear Stiffness for pinion

```
%% Shearing Stiffness
functionys = stiff_ks(a)
```

```
global E L mu a2v a1v index
if index ==1
    a1 = a1v(1);
    a2 = a2v(1);
elseif index ==2
    a1 = a1v(2);
    a2 = a2v(2);
elseif index ==3;
    a1 = a1v(3);
    a2 = a2v(1);
elseif index ==4
    a1 = a1v(4);
    a2 = a2v(2);
end
caln1 = 1.2*(1 + mu)*(a2 - a).*cos(a)*power(cos(a1),2);
caln2 = E*L*(sin(a) + (a2 - a)*cos(a));
ys = caln1./caln2;
```

Hertzian stiffness for Pinion

```
functionyh = stiff_kh(E,L,mu)

yh = pi/4*E*L/(1 - mu^2);

y = 1.2.*caln1./(cald1.*cald2);

%%
```

Pinion Single Meshing

```
function a11 = pinion_single_mesh(N1,N2,a0,theta1)
% A function to angular deflection
% theta1 - angular displacement of the pinion
cal0 = N1*cos(a0);
cal1 = (N2 + 2)^2 + (N1 + N2)^2 - 2*(N2 + 2)*(N1 +
N2)*cos(acos(N2*cos(a0)/(N2 + 2)) - a0);
cal2 = power(cal1,1/2);
cal3 = atan(cal0/cal2);

a0_inv = tan(a0) - pi*a0/180;
a11 = theta1 - pi/(2*N1) - a0_inv + tan(cal3);

%% Last line
cald2 = power(sind(a) + (1.37 - a).*cosd(a),2);

%%

y = 3.*caln1.*caln2./2.*(cald1.*cald2);
```

```
%%
```

Pinion Double Meshing

```
function a12 = pinion_single2_mesh(N1,N2,a0,theta1)
% A function to angular deflection
% theta1 - angular displacement of the pinion
cal0 = N1*cos(a0);
cal1 = (N2 + 2)^2 + (N1 + N2)^2 - 2*(N2 + 2)*(N1 +
N2)*cos(acos(N2*cos(a0)/(N2 + 2)) - a0);
cal2 = power(cal1,1/2);
cal3 = atan(cal0/cal2);

a0_inv = tan(a0) - pi*a0/180;
a12 = theta1 - 3*pi/(2*N1) - a0_inv + tan(cal3);

%% Last line
```

Gear Single Meshing

```
function a11p = gear_single_mesh(N1,N2,a0,theta1)
% A function to angular deflection
% theta1 - angular displacement of the pinion

cal0 = tan(acos(N2*cos(a0)/(N2 + 2)));

a0_inv = tan(a0) - pi*a0/180;
a11p = cal0 - pi/(2*N2) - a0_inv - N1/N2*theta1;

%% Last line
```

Gear Double Meshing

```
function a12p = gear_single2_mesh(N1,N2,a0,theta1)
% A function to angular deflection
% theta1 - angular displacement of the pinion

cal0 = tan(acos(N2*cos(a0)/(N2 + 2)));

a0_inv = tan(a0) - pi*a0/180;
a12p = cal0 - 5*pi/(2*N2) - a0_inv - N1/N2*theta1;

%% Last line
```

Meshing Duration

```
function [theta_d,theta_s] = mesh_duration(N1,N2,a0)
a0 = pi*a0/180;
```

```
cal0 = N1*cos(a0);
cal1 = (N2 + 2)^2 + (N1 + N2)^2 - 2*(N2 + 2)*(N1 +
N2)*cos(acos(N2*cos(a0)/(N2 + 2)) - a0);
cal2 = power(cal1,1/2);
cal3 = atan(cal0/cal2);
cal4 = tan(acos(N2*cos(a0)/(N2 + 2)));

theta_d = cal4 - 2*pi/N1 - tan(cal3);
theta_s = 2*pi/N1 - theta_d;

theta_d = 180*theta_d/pi;
theta_s = 180*theta_s/pi;

%% Last line
```

Main Program for Overall Meshing Stiffness

```
clearall; clc
% Main program

%% Inputs
global E L mu a2v a1v index

E = 2.068e+11;
mu = 0.3;
L = 16/1000; % width in meter

a0 = 20; % pressure angle on degree
N1 = 19;
N2 = 48;

%% Minimal pressure angle
x = linspace(4,100,100);
a0m = asind(sqrt(2./x));
figure (1)
plot(x,a0m,'k','LineWidth',1.5);xlabel('N_1');ylabel('\alpha_{0m}(^o)')

%% Mesh stiffness
a0_inv = tan(a0) - pi*a0/180;
a2 = pi/(2*N1) + a0_inv;
a2p = pi/(2*N2) + a0_inv;
a2v = [a2 a2p];
[theta_d,theta_s] = mesh_duration(N1,N2,a0);

theta1 = linspace(0,20,21);
for j = 1:length(theta1)
kh(j) = stiff_kh(E,L,mu); % Hertzian Stiffness

a11(j) = pinion_single_mesh(N1,N2,a0,theta1(j));
a12(j) = pinion_single2_mesh(N1,N2,a0,theta1(j));
```

```
a11p(j) = gear_single_mesh(N1,N2,a0,theta1(j));
a12p(j) = gear_single2_mesh(N1,N2,a0,theta1(j));

    a1v = [a11(j) a12(j) a11p(j) a12p(j)];
% ============================================== %
index = 1;
kb11(j) = 1./quad(@stiff_kb,-a11(j),a2); % first pair
ks11(j) = 1./quad(@stiff_ks,-a11(j),a2);
ka11(j) = 1./quad(@stiff_ka,-a11(j),a2);

index = 2;
kb21(j) = 1./quad(@stiff_kb,-a12(j),a2p); % second pair
ks21(j) = 1./quad(@stiff_ks,-a12(j),a2p);
ka21(j) = 1./quad(@stiff_ka,-a12(j),a2p);

index = 3;
kb12(j) = 1./quad(@stiff_kb,-a11p(j),a2);
ks12(j) = 1./quad(@stiff_ks,-a11p(j),a2);
ka12(j) = 1./quad(@stiff_ka,-a11p(j),a2);

index = 4;
kb22(j) = 1./quad(@stiff_kb,-a12p(j),a2p);
ks22(j) = 1./quad(@stiff_ks,-a12p(j),a2p);
ka22(j) = 1./quad(@stiff_ka,-a12p(j),a2p);
% ============================================== %
end
figure (2)
plot(theta1,kh)
```